International Journal of Heat and Mass Transfer 79 (2014) 532–550

Contents lists available at ScienceDirect

International Journal of Heat and Mass Transfer

journal homepage: www.elsevier.com/locate/ijhmt

A Coupled Level Set and Volume of Fluid method with multi-directional advection algorithms for two-phase flows with and without phase change

B.M. Ningegowda, B. Premachandran *

Department of Mechanical Engineering, Indian Institute of Technology Delhi, Hauz Khas, New Delhi 110016, India

ARTICLE INFO

Article history:
Received 26 March 2014
Received in revised form 16 July 2014
Accepted 17 August 2014

Keywords:
Level Set
Volume of Fluid
CLSVOF
Multi-dimensional advection
Film boiling

ABSTRACT

A Coupled Level Set and Volume of Fluid (CLSVOF) interface capturing method using a multi-dimensional advection algorithm for non-uniform grids has been developed for two phase flows with and without phase change for two-dimensional problems. A finite volume method with a collocated grid arrangement is used for solving the governing equations. The SIMPLE algorithm is used for velocity and pressure coupling. The piecewise linear interface calculation (PLIC) based geometrical reconstruction procedure and an Edge Matched Flux Polygon Advection (EMFPA) multi-dimensional algorithm have been implemented for the Volume of Fluid (VOF) method. For the Level Set (LS) advection equation, the convective terms are discretized using the second order accurate essentially non-oscillating (ENO) scheme. The proposed multi-dimensional advection of CLSVOF method requires interface reconstruction for the advection of VOF function and the Level Set function re-initialization only once compared to the requirement of twice interface reconstruction and Level Set re-initialization in the operator-splitting method for 2D problems. The performance of proposed CLSVOF method is evaluated for accurate mass conservation, surface tension force and interface mass transfer through various standard benchmark problems. The numerical study of two-dimensional saturated film boiling flow over a horizontal plane surface was carried out for different constant wall superheats in order to validate the implementation of boiling flow model. The present numerical results of boiling flows show better agreement with the experimental correlations.

1. Introduction

For modeling two-phase flows with sharp interfaces, the following methods are widely used: (a) interface fitting method (b) interface tracking method and (c) interface capturing method [1]. In the interface fitting (Lagrangian) method, the interface is treated as a sharp boundary and a moving mesh is used to follow the phase interface. However, this method cannot handle bubble breakup and coalescence [2]. Also, this method is computationally expensive due to the requirement of grid modification to follow the transient moving interface. In the interface tracking method, a fixed grid is used to obtain the velocity field and a moving surface mesh is used for interface tracking. In this method surface remeshing is required as the interface deforms [3]. Hence this method is computationally intensive and difficult to implement. In the interface capturing methods, the position of moving interface is captured in a fixed (Eulerian) grid based on an indication function. These methods can capture strong topological changes such as break up and merger of bubbles. These methods are computationally inexpensive and robust compared to the interface fitting and interface tracking methods. Hence, these methods are widely used in the numerical study of two-phase problems, with or without phase change. However, these methods may lead to poor mass conservation or inaccurate prediction of surface tension force. Many researchers have proposed various modifications in the interface capturing methods to overcome these problems.

Most commonly used interface capturing methods are the Level Set (LS), Volume of Fluid (VOF) and Coupled Level Set and Volume of Fluid (CLSVOF) methods. The LS method was first developed by Osher and Sethian [4] for the simulations of two-phase flows and further modified by Sussman et al. [5] for the simulations of two-phase flows. In this method, the moving interface is described through a smooth continuous LS function, ϕ. This function indicates a shortest signed distance from the interface, whose value is zero at the interface. Its value is negative in one fluid

* Corresponding author.
E-mail address: prem@mech.iitd.ac.in (B. Premachandran).

http://dx.doi.org/10.1016/j.ijheatmasstransfer.2014.08.039
0017-9310/

Nomenclatures

A_{F_T}	net advection flux of the cell, m^2
C_P	fluid specific heat at constant pressure, J/kg K
F	Volume of Fluid (VOF) or void fraction function
F_{st}	interfacial volumetric surface tension force, N/m^3
F_{sa}	interfacial surface tension stress, N/m^2
Gr	Grashof number
g	acceleration due to gravity, m/s^2
h_{lg}	latent heat of vaporisation, J/kg K
$H(\phi)$	smoothed Heaviside function
Ja	Jacob number
k	thermal conductivity of fluid, W/m K
m_I''	interfacial rate of mass flux, kg/m^2 s
$\overline{Nu}_{\lambda_d}$	local Nusselt number
$\overline{Nu}_L$	space averaged Nusselt number
$\overline{Nu}_T$	time averaged Nusselt number
$\vec{n}$	unit normal vector of the phase interface
P	pressure, Pa
Pr	Prandtl number
q_I''	interface heat flux, W/m^2
S_I	surface area (S_{cf}) of the interface line segment, m^2
S_C	surface of line segment bounded by the control volume cell, m^3
T	temperature, K
u, v	velocity components in x and y directions respectively, m/s
$\boldsymbol{V}$	velocity vector (u,v), m/s
V_I	interfacial velocity due to mass transfer, m/s

Greek symbols

α	thermal diffusivity, m^2/s
δ_s	Dirac surface delta function
ε	width of smoothed transition region, m
κ	interfacial local mean curvature, 1/m
λ	characteristic length scale for phase change, m
μ	dynamic viscosity of fluid, N s/m^2
ρ	density of fluid, kg/m^3
σ	surface tension coefficient, N/m
ϕ	continuous level set function

Subscripts

f	fluid phase
g	vapour or gas phase
I	liquid–vapour phase interface
l	liquid phase
Sat	saturation

Superscripts

n	previous time level
$n+1$	current time level

and positive in the other fluid. This method provides accurate unit normal vector, mean curvature and surface tension force of the interface. Implementation of this method is easy even for three-dimensional two-phase flows. The main drawback of this method is poor mass conservation which may lead to inaccurate capturing of dynamic interfaces.

In the VOF method, the moving interface is captured implicitly by a discontinuous VOF indicator function, F. In this method, the indicator function is zero in one fluid and one in the other fluid. At the interface cell, it vary between zero and one. Two approaches are used to solve the VOF Eq. (1) discretization of the volume fraction equation using anyone of high resolution schemes and (2) approximation of the interface geometrically in a two-phase cell using the void fraction, F. The first approach is easy to implement even for unstructured grids. However, this approach produces a highly diffusive interface and affects the accuracy of the solution. Hence, this approach is not preferred for the phase change problems and not discussed further. The second approach is the advection of volume fraction based on geometric interface reconstruction. This approach provides a sharp interface between two phases. The widely used interface reconstruction methods are SLIC (Simple Line Interface Calculation) [6] and PLIC (Piecewise Linear Interface Calculation) [7]. The VOF method has good mass conservative property, but computes the interfacial unit normal vector, mean curvature and surface tension force inaccurately. The inaccurate evaluation of the surface tension force across the interface may lead to the generation of spurious currents. In order to improve the solution, ELVIRA (Efficient Least squares Volume-of-fluid Interface Reconstruction Algorithm) [8] and PROST (Parabolic Reconstruction Of Surface Tension) [9] methods were introduced. Other methods which are limited to 2D flows are SIR (Spline-based Interface Reconstruction) [10] and QUASI (QUAdratic Spline based Interface) [11]. These methods are either difficult to implement or computationally expensive for both non-uniform structured grids and unstructured grids.

Various time integration schemes are used to solve the VOF function equation. The multidirectional un-split time integration scheme, as shown in Fig. 1(a), causes inaccuracy due to double fluxing problem [12]. The twice fluxing problem may lead to overshoot ($F > 1$) or undershoot ($F < 0$) of the VOF function, F in the computational domain. In order to avoid double fluxing problem, an operational split method [13] is used. In this method, at each time step, the advection equation of the VOF function is solved in each spatial coordinate direction as shown in Fig. 1(b) and (c) for the case of 2D problem. The geometric reconstruction of the interface has to be carried out before solving the advection equation in each spatial direction based on the VOF functions obtained from the solutions of the previous spatial direction advection. As the directional advection method required reconstruction of the interface twice and thrice for the 2D and 3D problems respectively this approach is computationally expensive and time consuming. Hence, Rider and Kothe [14] introduced a multi-dimensional (or un-split) advection algorithm for the VOF method to avoid the double fluxing as shown in Fig. 1(a). However, the twice (or double) fluxing problem could not be eliminated completely mainly due to an inaccurate geometrical construction of mass flux advection polygon at each control volume faces as shown Fig. 1(d). To avoid this problem in the solutions, Lopez et al. [10] developed the Edge Matched Flux Polygon Advection (EMFPA) algorithm for two-dimensional problems (Fig. 1(e)) and Hernandez et al. [15] and Lopez et al. [16] developed the Face Matched Flux Polyhedron Advection (FMFPA) algorithm for three-dimensional problems. Very recently, Tsui and Lin [17] introduced a multidirectional advection algorithm for the VOF method for non-orthogonal grids.

Taking positive aspects of both the VOF and the LS methods, the Combined Level Set and Volume of Fluid (CLSVOF) method was first proposed by Bourlioux [18]. Implementation of CLSVOF method by Sussman and Puckett [19] has popularised this method. The CLSVOF method is more accurate for the simulation of two-phase flows because of its better mass conservation, accurate

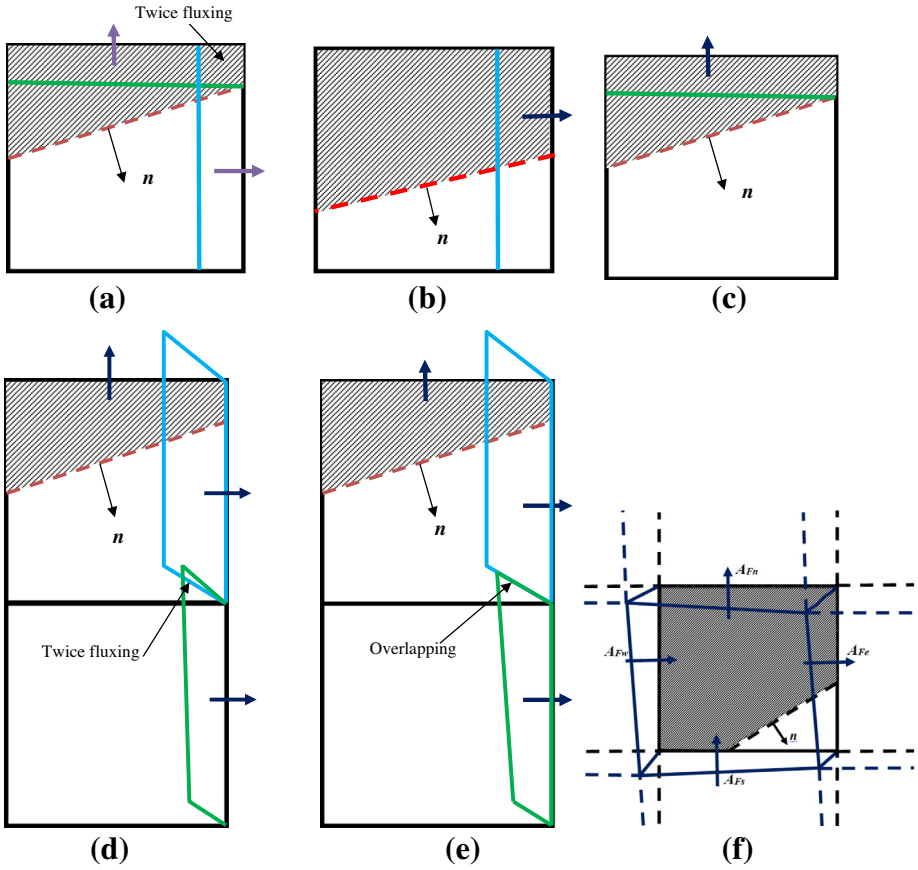

Fig. 1. Various VOF advection algorithms (a) Double flexing multi-directional advection, (b) operational split advection in x-direction, (c) operational split advection in y-direction, (d) multi-directional algorithm of Rider and Kothe [14], (e) EMFPA of Lopez et al. [10] and (f) edge matched flux polygons advection of the interface cell.

calculation of unit normal vectors, mean curvature and the surface tension force at the phase interface cells.

In almost all the existing CLSVOF methods, the VOF and LS advection equations are solved using the operational split (or fractional step) method [20–29] except Yang et al. [30] who used a Lagrangian–Eulerian method for the advection of VOF function. In the operational split method, at each time step the advection equations of both LS and VOF functions are solved in each spatial coordinate direction. The geometric reconstruction has to be carried out based on the LS and VOF functions obtained from the solutions of the previous spatial direction advection equations before solving advection equations in the next spatial direction. At each time step, the solution of advection equations requires additional computational power to carry out geometric reconstruction and re-initialization procedures. Therefore, at each time step the numerical study of 2D and 3D problems requires the solutions of advection equations, geometrical interface reconstruction and the LS re-initialization twice and thrice, respectively. These additional calculations of the interface capturing algorithms become computationally expensive and is not suitable for unstructured grid computational domains. Hence it is important to use a multi-directional advection algorithm in the CLSVOF method. A multi-directional advection algorithm in the CLSVOF method is possible only if accurate multidirectional advection algorithm is used to solve the advection equation of the VOF function.

Even though various multi-directional algorithms have been used for the VOF method, these algorithms are not used in the CLSVOF method till now. Implementation of a multi-direction advection for the CLSVOF method significantly reduces the computational time for the simulation of two-phase flows. In general, a multidimensional advection algorithm of a CLSVOF method reduces 50% and 66.67% of computational power requires for additional geometric reconstruction of the interface and the LS re-initialization algorithms needed at each time step for 2D and 3D problems, respectively. In the present work, a CLSVOF method is introduced with a multidirectional advection of both the VOF and the LS functions. For a multi-directional advection of VOF function, the EMFPA algorithm is used. In this study, various benchmark cases were considered for testing the advection algorithm, surface tension and phase change models to evaluate the performance of the proposed method.

The proposed CLSVOF method has also been extended to boiling flows to evaluate the performance of proposed interface capturing method for phase change problems. In the present study, the Stefan problem and film boiling over a horizontal surface are considered as test cases. Various methods have been used to simulate film boiling over a horizontal flat surface. This phase change problem was attempted by Son and Dhir [31,32] using a modified LS method. Juric and Tryggvason [33] developed a front tracking method to investigate film boiling flows using a single field formulation. Welch and Wilson [34] introduced a modified VOF method for investigating film boiling flows over a horizontal wall maintained at a uniform temperature. Welch and Rachidi [35] used the same approach of [34] to investigate film boiling over a finite thick plate with constant wall heat flux condition at the bottom of the plate. Agarwal et al. [36] investigated saturated film boiling of water at near critical conditions over an isothermal horizontal plane surface using the VOF method with ELVIRA to reduce spurious currents. Esmaeeli and Tryggvason [37,38] investigated multi-mode film boiling using a front tracking methods. Tomar

et al. [23] developed a CLSVOF method with uni-directional, operational split advection algorithm for saturated film boiling of water and the refrigerant R134a at near and far critical conditions at different wall superheat conditions. Gada and Sharma [39] simulated saturated film boiling of water using a dual grid LS method to avoid the mass loss problem. Recently, Tsui et al. [40] used a VOF method with a multi-directional advection method to simulate two-dimensional film boiling over flat and cylindrical surfaces.

Even though the CLSVOF method is effectively used for boiling flow problems, further improvement is required to reduce the computational time through a multi-directional advection instead of using a uni-directional advection algorithm. Using a non-uniform grid would help us to capture the gradient of any variable accurately with relatively less number of grid points without affecting the accuracy of the solution. The reduction of number of control volumes in the computational domain using a non-uniform grid size further reduces the requirement of the computational power. Hence, in the present study a new CLSVOF method is proposed for non-uniform grids with the Edge Matched Flux Polygon Advection (EMFPA) based multi-dimensional advection algorithm, which requires the geometric interface reconstruction, advection and re-initialization of the LS function only once at each time step has been presented. The performance of the proposed method has been evaluated for various standard test cases including phase change problems and the results obtained from these studies are presented in this paper.

2. Governing equations for two phase flows with or without phase change

In this subsection, the governing equations for two-phase flows, with and without phase change are presented. In the case of two-phase flows, the surface tension force is included as a source term in the momentum equations for the interface cells. Additional modifications are also required to account heat and mass transfer across the interface for two-phase flows with phase change problems. In the first sub-section, the governing equations related to two-phase flow problems without phase change are provided. For phase change problems, boiling flows are considered in the present study. The governing equations for boiling flows are presented in the second sub-section.

2.1. Governing equations used for two phase flow without phase change

The continuity equation for incompressible flow is written as,

$$\nabla \cdot V = 0 \tag{1}$$

The momentum transport equation for single phase cell is written as

$$\rho_f \left(\frac{\partial V}{\partial t} + V \cdot \nabla V \right) = -\nabla P + \nabla \cdot \mu_f \left[\nabla V + (\nabla V)^T \right] + \rho_f g \tag{2}$$

where, the superscript T indicates the transpose operation of diffusion terms. The term in the above equation, $\nabla \cdot \mu_f[\nabla V + (\nabla V)^T]$ indicates the rate of deformation.

For liquid–vapour interface cell region, the momentum Eq. (2) is modified as

$$\rho_f \left(\frac{\partial V}{\partial t} + V \cdot \nabla V \right) = -\nabla P + \nabla \cdot \mu_f [\nabla V + (\nabla V)^T] + \rho_f g + F_{st} \tag{3}$$

The interfacial surface tension force per unit volume, F_{st} is computed as $F_{st} = F_{sa}\delta_s$. The surface tension force per unit interfacial area, F_{sa} is the sum of the normal and tangential surface tension stress components. It is computed as $F_{sa} = f_n + f_t$, where, $f_n = \sigma\kappa\vec{n}$ and $f_t = \partial\sigma/\partial x_i$ are the normal and tangential stress components at the interface segment. The surface tension coefficient, σ is taken to be a constant due to negligible variation of σ with temperature and concentration [23,24,34]. Hence, the tangential surface stress component, f_t becomes zero. The net interfacial surface tension stress can be written as, $F_{sa} = \sigma\kappa\vec{n}$ and volumetric interfacial surface tension force is expressed as $F_{st} = \sigma\kappa\vec{n}\delta_s$

2.2. Governing equations used for two phase flow with phase change problems

In the present work, 1-D Stefan problem and 2-D saturated film boiling over a horizontal flat plate are considered for the validation of the phase change model developed using the proposed CLSVOF method with multidimensional advection algorithm. In this sub-section, the governing equations used for the simulation of saturated boiling flows are presented.

For boiling flows, the continuity Eq. (1) should be modified in order to account mass transfer across the interface. The modified continuity equation for the interface cells can be written [23,34,36] as

$$\int_{S_c} V \cdot \vec{n} ds + \int_{S_{I(t)}} \left(\frac{1}{\rho_l} - \frac{1}{\rho_g} \right) \frac{\|q_I''\| \cdot \vec{n}}{h_{\mathrm{lg}}} ds = 0 \tag{4}$$

The second term in the above equation accounts for the interface mass transfer due to phase change. This term is non-zero only at the interface.

In the case of saturated film boiling, the energy equation is solved in only the superheated vapour region. The energy equation for superheated vapour phase region can be written as

$$\rho_f C_{Pf} \left(\frac{\partial T}{\partial t} + V \cdot \nabla T \right) = \nabla \cdot k_f (\nabla T) \tag{5}$$

In saturated boiling flows, the solution of the energy equation is not required for the saturated liquid phase and interface cell regions. At the interface region, the cell centre temperature is extrapolated based on the adjacent superheated vapour cell normal to the interface using an array of nine-point stencil [33,34].

In the case of two-phase flows with phase change, the thermophysical properties of fluids are discontinuous at the interface [19]. To avoid numerical instability [20], fluids properties such as density, viscosity, specific heat and thermal conductivity are evaluated in terms of the smoothed Heaviside function, $H(\phi)$. Any material properties of fluid, γ_f can be computed in terms of $H(\phi)$ as

$$\gamma_f = \gamma_g + (\gamma_l - \gamma_g) H(\phi) \tag{6}$$

The smoothed Heaviside function, $H(\phi)$ in the whole computational domain [20] is computed as

$$H(\phi) = \begin{cases} 1 & \textit{Liquid phase, if } \phi > \varepsilon \\ 0.5 + \left(\frac{\phi}{2\varepsilon}\right) + \frac{1}{2\pi} \sin\left(\frac{\pi\phi}{\varepsilon}\right) & \textit{Interface, if } |\phi| \leqslant \varepsilon \\ 0 & \textit{Vapour phase, if } \phi < \varepsilon \end{cases} \tag{7}$$

where, ε is the width of the interface region and is calculated in terms of the domain grid size using the expression as, $\varepsilon = 3(\Delta x_c + \Delta y_c)/4$. Here Δx_c and Δy_c are the width and height of the non-uniform cell size.

3. CLSVOF method with multidimensional advection algorithms

As discussed in the introduction section, CLSVOF methods were widely developed for the uniform grid with operator-split advection algorithm except Yang et al. [30] who developed a CLSVOF method for simulating two phase flows using unstructured triangular grids. In the operator-split advection algorithm, the

VOF geometrical interface reconstruction and the LS re-initialization procedures have to be carried out twice or thrice depending on whether the problem is 2D or 3D. Using a multidirectional advection algorithm one can avoid the additional time consuming interface reconstruction and re-initialization procedures of unidirectional advection.

In the present CLSVOF study, the VOF based multi-dimensional advection equation is solved using the EMFPA algorithm of Lopez et al. [10]. In the VOF method, a discrete volume fraction function, F is initialized in the computational domain. The value of F is unity for the cell completely filled with the discrete phase and zero for the cell completely filled with the continuous phase. In the interface cell, F varies between zero and one. The transient motion of the phase interface is obtained by solving the VOF advection equation [10] as

$$\frac{\partial F}{\partial t} + (V \cdot \nabla)F = 0 \tag{8}$$

The advection Eq. (8) can be re-written as

$$\frac{\partial F}{\partial t} + \nabla \cdot (VF) = F(\nabla \cdot V)$$

Using the continuity equation (Eq. (1)), the above-mentioned advection equation can be written as

$$\frac{\partial F}{\partial t} + \nabla \cdot (VF) = 0 \tag{9}$$

For boiling flows, the above VOF equation is modified as

$$\frac{\partial F}{\partial t} + \nabla \cdot (VF) = F_{mt} \tag{10}$$

where, F_{mt} is rate of volume fraction generated due to the interfacial mass transfer. This mass transfer takes place due to phase change occurs between the liquid–vapour interfaces. For VOF-PLIC based analytical geometrical interface reconstruction, the algorithm introduced by Lopez and Hernandez [41] is used. The VOF advection Eq. (10) can be discretized explicitly as,

$$F^{n+1} = F^n - \frac{1}{V_\Omega}\int_{t_n}^{t_{n+1}}\int_\Omega \nabla \cdot (VF)d\Omega dt + F_{mt}\Delta t \Delta\Omega \tag{11}$$

The second term in the RHS indicates the net area of the fluid element, A_{F_T} which is advected out of the each computational cell. This can be computed as $A_{F_T} = A_{Fs} + A_{Fe} + A_{Fn} + A_{Fw}$ in the domain as shown in Fig. 1(f). The amount of fluid leaving out of the cell through its edge face is taken as positive and the amount of fluid entering into the cell is taken as negative [10].

In the LS method, the moving interface is captured by solving the advection equation of the level set function, ϕ. The LS function indicates a shortest distance from the interface to the centre of each computational cell in the domain. The value of level set function, ϕ is positive if the cell is completely filled with continuous phase ($\phi > 0$), is negative if the cell is completely filled with discrete phase ($\phi < 0$), and is zero at the phase interface ($\phi = 0$). For simulating two-phase flows, the LS advection equation [20] can be written as

$$\frac{\partial \phi}{\partial t} + (V \cdot \nabla)\phi = 0 \tag{12}$$

The LS advection Eq. (12) is modified for the phase change problem [31] as

$$\frac{\partial \phi}{\partial t} + (V_{mt} \cdot \nabla)\phi = 0 \tag{13}$$

where, $V_{mt} = V_{cell} + V_I\vec{n}$. Here, V_{cell} is the cell centre velocity field and $V_I = v_{lg}m_I''$ is the interfacial velocity due to mass transfer across the phase interface.

3.1. VOF-PLIC based geometrical interface reconstruction algorithm

In the CLSVOF method, the interface normal vector, $\vec{n}$ is accurately calculated based on the LS function as,

$$\vec{n} = \frac{\nabla\phi}{|\nabla\phi|} \tag{14}$$

The orientation of the phase interface position is computed in terms of normal vector $\vec{n}$. The derivative of the LS function is discretized using the second order accurate central difference scheme (CDS) using an array of 3×3 (or nine-point stencil) cells. The unit normal vector computed in terms of the continuous LS function, ϕ is more accurate as compared to that of discrete VOF function, F. From the known interface unit normal vector and the VOF function, F, the interface position is geometrically reconstructed using the Piecewise Linear Interface Calculation (PLIC) method. In the VOF-PLIC based geometric reconstruction method, a moving interface is approximated as a straight line within a mixed cell and is defined as, $\vec{n} \cdot \vec{X} + C = 0$ .The unit normal vector, $\vec{n}$ is pointing towards the continuous phase. Here, $\vec{X}$ is the position vector of a generic point on the interface line and C is the interface line constant. In the PLIC based reconstruction algorithm, the position of a moving interface is computed analytically using two basic operations, (a) volume truncation and (b) enforcement of the local volume conservation procedure introduced by Lopez and Hernadise [41].

3.2. Calculate the interfacial surface tension force

The governing equations in the interfacial cells are modified to include the surface tension force across the interface. To compute the interfacial surface tension force, various surface tension models are used. Important models are (a) Continuous Surface tension Force (CSF) model [42,43], (b) Continuous Surface tension Stress (CSS) model [44], (c) Parabolic Reconstruction Of Surface Tension (PROST) model [9], (d) CLSVOF method with CSF model [24] and (e) CLSVOF with pressure boundary method (PBM) model [29]. Among these models, the CSF based surface tension model is most widely used. In the present study, the CLSVOF-CSF model is used to calculate surface tension force. In this model, the interfacial volumetric surface tension force is computed as $F_{st} = \sigma\kappa\nabla H(\phi)$. The calculation of local mean curvature, κ based on continuous LS function is more accurate than that of discrete VOF function [20]. Therefore, the interfacial surface tension force calculation based on the LS function generates lesser parasitic currents as compared to the VOF function approach [24,26]. The local mean curvature, κ of the interface line segment is calculated using the expression

$$\kappa = -\nabla \cdot \left(\frac{\nabla\phi}{|\nabla\phi|}\right) = -\left(\frac{\phi_y^2\phi_{xx} - 2\phi_x\phi_y\phi_{xy} + \phi_x^2\phi_{yy}}{(\phi_x^2 + \phi_y^2)^{\frac{3}{2}}}\right) \tag{15}$$

In the above mean curvature Eq. (15), the first and second derivatives of LS functions are discretized using the standard second order accurate central difference scheme (CDS).

4. Numerical solution procedure

In this numerical study, two-dimensional governing equations are solved using a finite volume method with a collocated grid arrangement. The proposed two-phase flow solver is developed for non-uniform grids. The SIMPLE algorithm is used for velocity and pressure coupling. The convective terms of both momentum and energy transport equations are discretized using the QUICK scheme [45,46]. The diffusion terms of the momentum and energy equations are discretized using the second order accurate central differencing scheme (CDS). The unsteady terms are discretized

using the first order accurate explicit scheme. The time step constraints of an explicit scheme for the two-phase flow problems are extensively discussed in [47]. These constraints account the effect of convective, viscous, gravity and surface tension terms. The selected time step size, Δt should be always lower than the above mentioned constraints. The convective terms of the LS advection equation are discretized using the second order accurate essentially non-oscillatory (ENO) scheme introduced in [19,23]. The LS function is re-initialized using the geometric details available from the PLIC based interface reconstruction similar to [19,20].

5. Results and discussion

The performance of the proposed multidimensional advection algorithms of CLSVOF method developed for the two-phase flows without and with phase change is evaluated using various standard benchmark problems for the advection algorithm, the surface tension model and the phase change model for boiling flows. To evaluate the proposed CLSVOF method, the results obtained from the present study were compared with those of existing models and detailed analysis of these results are presented in the following subsections.

5.1. Benchmark problems of advection and geometric reconstruction algorithms

In the present study, performance of the proposed multidirectional advection algorithm is assessed qualitatively and quantitatively. The quantitative assessment is carried out in terms of the numerical error norms with different CFL numbers. The CFL number, C is calculated based on the maximum analytical velocity field in the domain as, $C = |U_{max}|\Delta t/\Delta x$. The error norms of L_1 and L_2 are computed in terms of VOF function, F in the computational domain [14,47]. Evaluation of proposed advection and geometrical reconstruction algorithms are discussed in the following subsections.

5.1.1. Rotation of Zalesak's slotted circular disk test

In this test, Zalesak's slotted circular disk revolves with respect to the centre of the computational domain. In this test, a circular bubble of radius, $r = 0.15$ m is initially positioned at the centre (0.5 m, 0.75 m) with a rectangular slot of width, $a = 0.05$ m and height, $b = 0.25$ m is placed in the unit square domain is shown in Fig. 2(a). A spatially varying velocity field is prescribed analytically as, $u = \frac{\pi}{3.14}\left(\frac{1}{2} - y\right)$ and $v = \frac{\pi}{3.14}\left(x - \frac{1}{2}\right)$.

In this test case, the geometry of the slotted disk obtained after one complete rotation at CFL number, $C = 0.25$ using the proposed CLSVOF method is compared with the initial geometry for non-uniform grids. At higher CFL numbers and coarse grids, slight change in the shape of the initial geometry occurs due to the limitations of the interface reconstruction and advection algorithms. The sharp corners are smoothed out due to the linear geometrical reconstruction of the interface. The difference between the numerical reconstruction and the exact geometry is visible only in the small regions near the sharp corners of the disk. The shape obtained from the proposed CLSVOF method is qualitatively good agreement with the CLSVOF results of Wang et al. [28] are shown in Fig. 2(b) and (c), respectively. Wang et al. [28] have not presented their results quantitatively. Considering this problem as one of the test case, Lopez et al. [10] carried out a detailed comparative study on the performance of various geometric reconstruction and advection algorithms. The relative error (or L_2 norms) obtained from the present CLSVOF method is compared with those of Lopez et al. [10] in Table 1 for the CFL number, $C = 0.25$ and the grid size of 100×100. The relative error obtained from the proposed CLSVOF method is less than that of various advection/reconstruction algorithms investigated in [10].

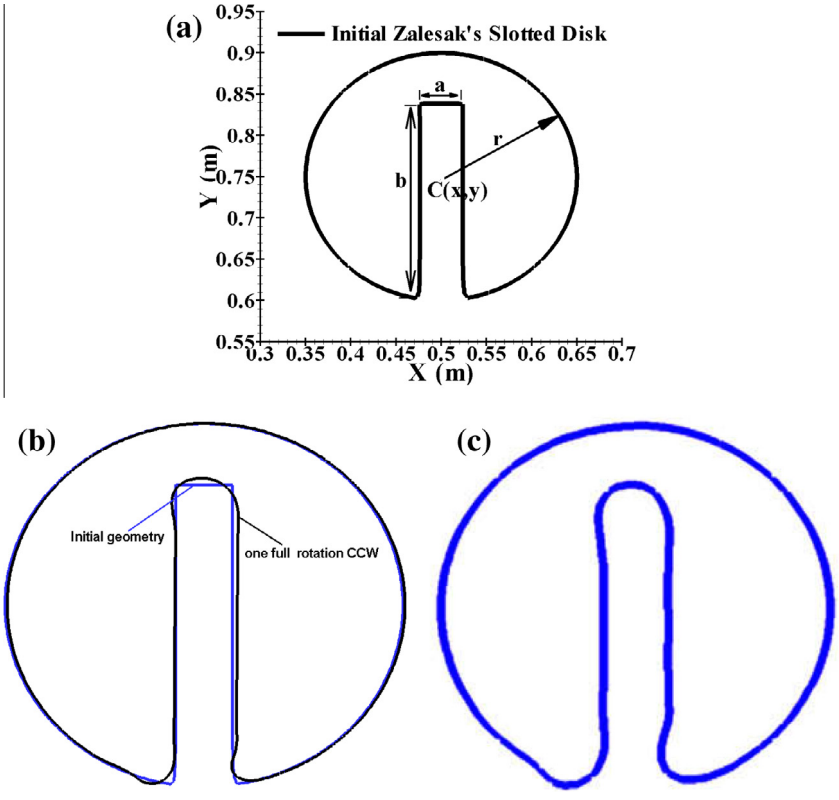

Fig. 2. Rotation of Zalesak's slotted disk (a) initial geometry, (b) comparison of present CLSVOF method with CLSVOF method of Wang et al. [28].

Table 1
Comparison of the L_2 (relative) error norms of Zalesak's slotted circular disk after one complete rotation using various interface reconstruction/advection algorithms.

Sl. no	Advection or reconstruction algorithms	L_2 (relative) error norms
1	Youngs [7]	1.09×10^{-2}
2	Harvie and Fletcher [48] (Stream)/Youngs	1.07×10^{-2}
3	Harvie and Fletcher [48] (Stream)/Pucket	1.00×10^{-2}
4	Harvie and Fletcher [49] (DDR)/Youngs	1.56×10^{-2}
5	Harvie and Fletcher [49] (DDR)/Pucket	1.50×10^{-2}
6	Lopez et al. [10] EMFPA/Youngs	1.06×10^{-2}
7	Lopez et al. [10] EMFPA/Pucket	9.73×10^{-3}
8	Lopez et al. [10] EMFPA-SIR	8.74×10^{-3}
9	Scardovelli and Zaleski [50] (Linear least square fit)	9.42×10^{-3}
10	Scardovelli and Zaleski [50] (Quadratic fit)	5.47×10^{-3}
11	Scardovelli and Zaleski [50] (Quadratic fit + continuity)	4.16×10^{-3}
12	Present unsplit CLSVOF method	2.211×10^{-3}

5.1.2. Shear or single vortex flow test

As the interface does not undergo any topological change in the rotation test cases, this test case is not adequate to assess the performance of interface capturing methods [14,24]. Single vertex in a shear flow was considered as one of the test cases by [10,14,49] to evaluate their advection algorithms for the cases of strong interface deformation. In this test, a circular fluid body of radius, $r = 0.15$ m is initially placed at the centre point (0.5 m, 0.75 m) in a computational domain size of 1 m × 1 m. At all the domain boundaries, periodic boundary condition is imposed. Velocity field for the shear flow is prescribed analytically as

$$u = \sin^2(\pi x)\sin(2\pi y)\cos\left(\frac{\pi t}{T}\right) \quad \text{and}$$
$$v = -\sin^2(\pi y)\sin(2\pi x)\cos\left(\frac{\pi t}{T}\right) \tag{16}$$

where t is the time at any instant and T is the time at which the circular fluid body returns back to its initial shape.

Fig. 3(a) and (b) show the interface topologies obtained using the CLSVOF method of Wang et al. [28] and the present method, respectively, using a grid size of 128 × 128 at time $t = 3$ s. The shape obtained from the present study matches well with those of [28]. Lopez et al. [10] compared the absolute errors (L_1 norm) obtained using various reconstruction and advection algorithms for the time reversed test case for $T = 8$ s with the grid size of 128 × 128 for CFL = 1.0. Along with these results, the absolute error obtained based on the present CLSVOF method is compared in Table 2. The numerical error obtained using the present CLSVOF method is slightly higher than the advection algorithms investigated in [10].

A comparative study was also carried out with the values obtained from the CLSVOF method implemented by Gerlach et al. [24] for the velocity distribution, $u = sin(x)cos(y)$ and $v = -cos(x)sin(y)$. In their study, they considered a circle of radius, $\pi/5$ m placed at ($\pi/2$ m, $\pi/4$ m) in a square computational domain size of $\pi \times \pi$ m^2 and is discretized using the grid size of 100 × 100 cells. Numerical simulations were carried out using the CFL number, $C = 0.25$. Gerlach et al. [24] obtained relative errors (or L_2 norms) after 1000 time steps forward flow and after another 1000 steps backward flow from their CLSVOF method with unidirectional advection algorithm and their implementation of Youngs, LVIRA, PROST and Youngs (Rudman) methods. In Table 3, the relative errors occur from these methods are compared with the proposed CLSVOF method. This comparison shows that the proposed CLSVOF method performs better than the other methods listed in Table 3. The interface topologies obtained for 1000Δt forward flow followed by 1000Δt backward flow by Gerlach et al. [24] and the present CLSVOF method are shown in Fig. 3(c) and (d), respectively. These figures show that the proposed CLSVOF method

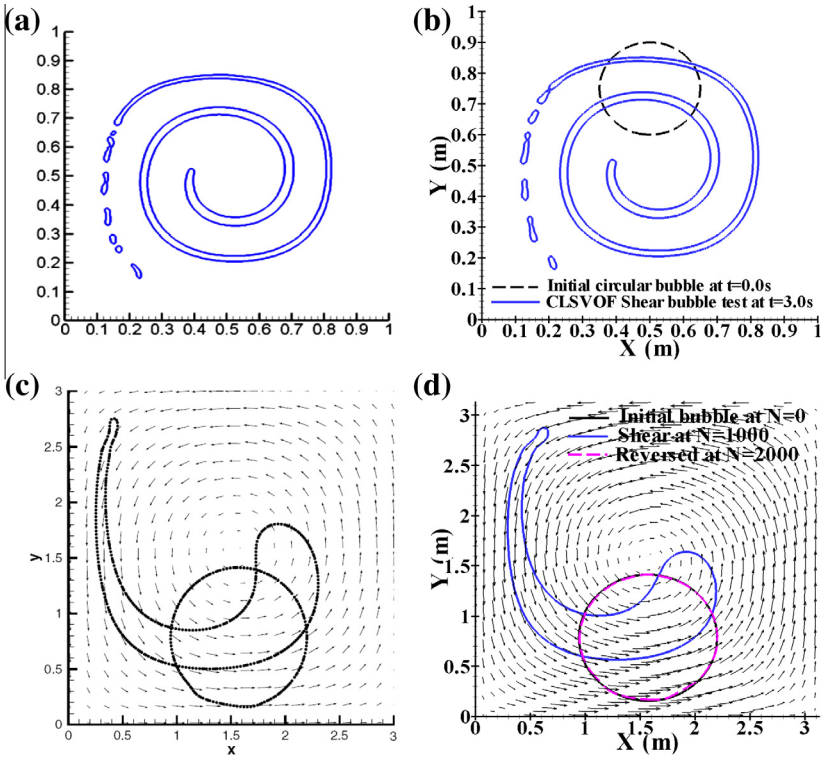

Fig. 3. Shear flow test (a) CLSVOF method of Wang et al. [28] (case 1), (b) proposed un-split CLSVOF method (case 1), (c) CLSVOF method of Gerlach et al. [24] (case 2), (d) proposed un-split CLSVOF method (case 2).

Table 2
Comparison study of L_1 (absolute) error norms of reversed shear flow at time, $t = 8$ s and CFL = 1 in a unit square computational domain.

Advection/reconstruction algorithm	L_1 (absolute) error norms
Rider and Kothe [14]	1.44×10^{-3}
Harvie and Fletcher [48]/Youngs	2.16×10^{-3}
Harvie and Fletcher [49]/Puckett	1.18×10^{-3}
Lopez et al. [10] EMFPA/Youngs	2.13×10^{-3}
Lopez et al. [10] EMFPA/Puckett	1.17×10^{-3}
Lopez et al. [10] EMFPA-SIR	7.57×10^{-4}
Proposed Un-Split CLSVOF method	3.9236×10^{-3}

with multi-directional advection algorithm compares well with the CLSVOF method with unidirectional advection algorithm of [24].

5.1.3. Deformation of the circular bubble test

This benchmark problem is one of the stringent tests for an advection algorithm for two-phase flows. This test was used to evaluate the performance of the advection algorithms developed by [14,51]. In this test, a circular bubble of radius, $r = 0.15$ m is initially placed at the centre (0.5 m, 0.5 m) of a unit square domain. All boundaries are imposed as periodic boundaries. The periodic, non-uniformly varying spatial complex deformation velocity field is prescribed analytically in the domain as

$$u = sin\left[n\pi\left(x+\frac{1}{2}\right)\right]\sin\left[n\pi\left(y+\frac{1}{2}\right)\right] \quad \text{and}$$
$$v = \cos\left[n\pi\left(x+\frac{1}{2}\right)\right]\cos\left[n\pi\left(y+\frac{1}{2}\right)\right] \tag{17}$$

where, n is the number of symmetrical $n \times n$ array of counter-rotating vortices in the domain. In the present study, vertices number, n is taken as 4 and the corresponding total number of counter-rotating vortices in the whole domain is 16. The maximum velocity in the domain is 1.0 m/s. In the time reversed test, the deformed circular bubble regains its initial geometry. In the time reversed deformation test, the velocity field is obtained by multiplying, $\cos(\pi t/T)$ to the above expressions (17). In this term, t is time at any instant and T is the total time at which the deformed bubble reversed back to its original shape.

For this test, both uniform and nonuniform grids are used in the present study. Fig. 4(a) shows the computational domain with a non-uniform grid size of 128×128. The interfaces obtained after 0.5 s forward flow followed by 0.5 s reverse flow are shown in Fig. 4(b) and (c) for the uniform and nonuniform grids, respectively. Similar plots for time, $t = 1.0$ s forward flow followed by 1.0 s reverse flow are shown in Fig. 4(d) and (e) for uniform and non-uniform grids, respectively. The two-phase flow pattern obtained with the nonuniform grid shows fewer breakups compared to the uniform grid. Rider and Kothe [14] and Garrioch and Baliga [51] used this test case to evaluate the performance of their PLIC-VOF method at the CFL number, $C = 0.25$ for the uniform grid size of 128×128. The absolute numerical error obtained for the uniform grids by Rider and Kothe [14], Garrioch and Baliga [51] and the present CLSVOF method are 5.95×10^{-3}, 4.66×10^{-3} and 4.213×10^{-4} respectively. These results show that the present CLSVOF method perform better compared to those of [14,51].

Table 3
Comparison of relative errors obtained for shear flow test using the proposed CLSVOF method with different methods of Gerlach et al. [24] at CFL = 0.25 at different numbers of iterations, N.

Author	Methods	E ($N = 1000$)	E ($N = 2000$)
Gerlach et al. [24]	Youngs	8.39×10^{-3}	3.73×10^{-2}
	LVIRA	6.55×10^{-3}	3.34×10^{-2}
	CLSVOF	5.08×10^{-3}	2.65×10^{-2}
	PROST	6.22×10^{-3}	3.19×10^{-2}
	Youngs (Rudman)	8.60×10^{-3}	3.85×10^{-2}
Proposed unsplit CLSVOF method		4.94×10^{-3}	2.14×10^{-2}

5.2. Evaluation of two-phase flow model with surface tension force

After the accuracy of the advection and reconstruction algorithms of the proposed CLSVOF method are evaluated, the performance of interface surface tension force is carried out. In the present study, CSF based surface tension model has been used for simulating two-phase flows. The static bubble test, dam break problem, Rayleigh–Taylor instability and a rising gas bubble inside a quiescent liquid column were widely used as benchmark test cases for two-phase flows. In these problems, the complexity arises due to the unavailability of analytical solutions for the velocity field. All the above mentioned cases were considered to evaluate the proposed method.

5.2.1. Static bubble test

This test is widely used to evaluate the performance of any surface tension model implemented in a numerical model of two phase flows. In this test, the effect of acceleration due to gravity and the other external forces are neglected. The initial velocity field in the whole computational domain is assumed to be zero. At equilibrium, the surface tension force is balanced by the pressure force which results in a pressure jump condition at the interface. This condition is specified using the Laplace equation, $P_{drop} = \sigma\kappa$, where, κ is the interface mean curvature and is analytically computed as the reciprocal of the radius of circle, R and σ is the surface tension coefficient. Ideal pressure distribution inside the bubble should be constant and is exactly balanced by the interfacial surface tension force. Simulation of this test case generates spurious currents which are mainly due to the inaccurate predictions of interfacial surface tension force.

Gerlach et al. [24] evaluated their CLSVOF-CSF model with the PROST and K_8 models. In the present study the same test case was considered to evaluate performance of the proposed CLSVOF-CSF model. In this test, the density ratios of 2 and 1000 are considered. A circular bubble of radius, $R = 2$ cm is placed at the centre of the square domain of size 6 cm $\times$ 6 cm. The effect of grid size in the generation of the parasitic currents is investigated for the uniform grid sizes of 30^2, 60^2 and 120^2. Using the present CLSVOF-CSF surface tension model, the L_1 and L_2 error norms, the maximum velocity in the computational domain and the ratio of average pressure to the pressure drop are obtained after 1 and 50 iterations and compared with those of Gerlach et al. [24] in Table 4. These results show that for both density ratios, the magnitudes of spurious currents obtained using the PROST model is lower than the K_8 and the CLSVOF based models. With grid refinement, the magnitudes of spurious currents increases with iterations for all the above mentioned surface tension models. However, Renardy and Renardy [9] highlighted that with grid refinement, for uniform density and viscosity of both fluids, the magnitude of spurious currents increases for both VOF-CSS and VOF-CSF based surface tension models and is decrease for the VOF-PROST based surface tension model.

Wang and Tong [29] studied a two-dimensional static bubble problem to evaluate the surface tension models, CLSVOF-CSF and their pressure boundary method (PBM) using three different density ratios of 1, 100 and 1000 with constant dynamic viscosity ratio of 10. To evaluate the proposed two-dimensional CLSVOF-CSF based surface tension model, the test case of Wang and Tong [29] is also considered. To investigate the effect of grid dependent spurious currents formation using a uniform grid size of 20^2, 40^2,

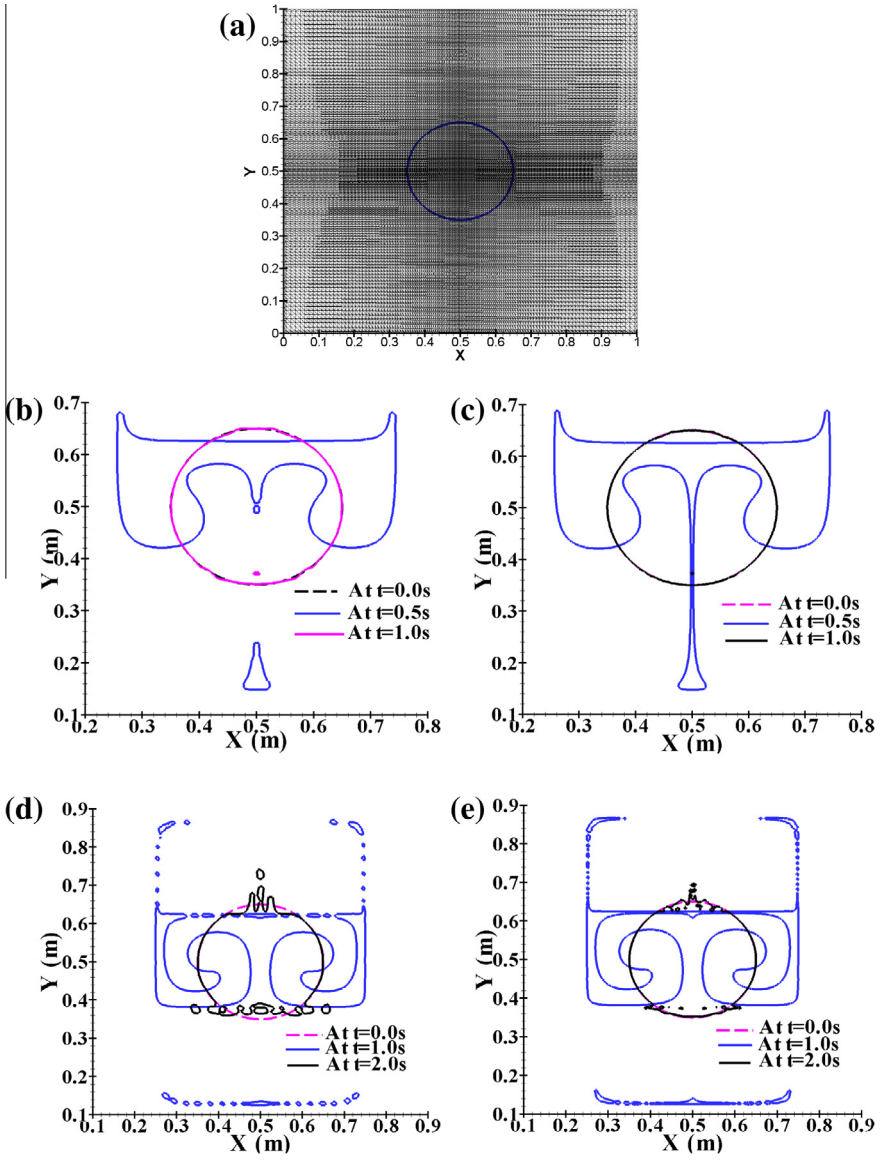

Fig. 4. Time reversed deformation test (a) non-uniform grid used, (b) at 0.5 s forward flow and 0.5 s backward flow with uniform grid, (c) at 0.5 s forward flow and 0.5 s backward flow with non-uniform grid, (d) at 1.0 s forward flow and 1.0 s backward flow with uniform grid and (e) at 1.0 s forward flow and 1.0 s backward flow with non-uniform grid.

80^2 and 160^2 are used. A constant time step, Δt of 10^{-5} s is used for all the above mentioned grids. The transient mean velocity in the domain obtained from present study for the density ratio of 1.0 and viscosity ratio of 10 are compared with the CLSVOF-PBM of Wang and Tong [29] for three different grid sizes at time $t = 0.5$ ms shown in Fig. 5(a). The proposed CLSVOF-CSF method results show that the mean velocity of the spurious currents increases with grid refinement as it was observed by [29]. However, in the case of CLSVOF-PBM method, the magnitudes of false velocity decreases with grid refinement and at higher grid sizes, the mean velocity is significantly lower than the CLSVOF-CSF method. The magnitudes of false velocity with different grids and density ratios are also evaluated in terms of the CFL number are presented in Fig. 5(b). From these results, it is found that the magnitude of spurious currents increases as the density ratio increases from 1 to 100. Further increase in the density ratio from 100 to 1000, there is no significant change in the magnitude of spurious currents. The same trend was also observed by Wang and Tong [29] with their pressure boundary method (PBM).

5.2.2. Dam break problem

In this test, a rectangular column of water collapses suddenly over a horizontal surface under the action of gravity. Initially, a water column of height, $b = 0.9$ m and width, $a = 0.45$ m is specified in a rectangular domain size of 2.0 m $\times$ 1.0 m. Numerical simulations were carried out for the grid size of 256×128. When the water column collapses under the action of gravity, the water wave front propagates towards the right side of the domain. Finally, it hits against the vertical right side wall and turns back to form a reverse wave and then starts rising upward along the right side wall. L and H are the transient interface positions of water and air interface along the bottom and left walls, respectively. The non-dimensional positions of the moving water wave front along the bottom wall (L/a) and the left vertical height of the water

Table 4
Comparison of the present CLSVOF-CSF results with the different surface tension models of Gerlach et al. [24] for density ratios of 2 and 1000 at time step, $\Delta t = 10^{-5}$ s.

Author	Method	R/dx	|Umax, 1|	|Umax, 50|	$(\langle P\rangle/P_{drop})$	L_1	L_2
Density ratio = 2.0							
Gerlach et al. [24]	PROST	20	1.14×10^{-7}	5.69×10^{-6}	1.00	7.18×10^{-4}	3.02×10^{-3}
	K_8		7.45×10^{-7}	3.59×10^{-5}	0.9844	1.56×10^{-2}	5.72×10^{-2}
	CLSVOF		9.69×10^{-7}	4.71×10^{-5}	0.995	4.83×10^{-3}	3.84×10^{-2}
	Brackbill		–	–	1.016	–	2.82×10^{-2}
Present CLSVOF-CSF			9.73×10^{-7}	4.87×10^{-5}	0.9874	4.68×10^{-3}	3.76×10^{-2}
Density ratio = 1000							
Gerlach et al. [24]	PROST	10	7.82×10^{-8}	3.91×10^{-6}	1.00	4.81×10^{-3}	4.83×10^{-3}
		20	1.70×10^{-7}	8.53×10^{-6}	1.00	9.48×10^{-4}	9.79×10^{-4}
		40	4.34×10^{-7}	2.17×10^{-5}	1.00	7.04×10^{-5}	5.25×10^{-4}
	K_8	10	2.28×10^{-6}	1.12×10^{-5}	0.978	2.17×10^{-2}	7.60×10^{-2}
		20	5.33×10^{-6}	2.66×10^{-4}	0.987	1.33×10^{-2}	4.90×10^{-2}
		40	4.62×10^{-5}	2.31×10^{-3}	0.988	1.19×10^{-2}	3.86×10^{-2}
	CLSVOF	10	1.16×10^{-6}	5.68×10^{-5}	0.989	1.14×10^{-2}	4.99×10^{-2}
		20	5.97×10^{-6}	2.92×10^{-4}	0.993	7.53×10^{-3}	3.17×10^{-2}
		40	1.91×10^{-5}	9.37×10^{-4}	0.997	2.92×10^{-3}	2.22×10^{-2}
Present CLSVOF-CSF		10	1.12×10^{-6}	5.11×10^{-5}	0.981	1.14×10^{-2}	4.04×10^{-2}
		20	5.88×10^{-6}	3.10×10^{-4}	0.987	7.53×10^{-3}	3.74×10^{-2}
		40	1.30×10^{-5}	9.43×10^{-4}	0.993	2.92×10^{-3}	2.46×10^{-2}

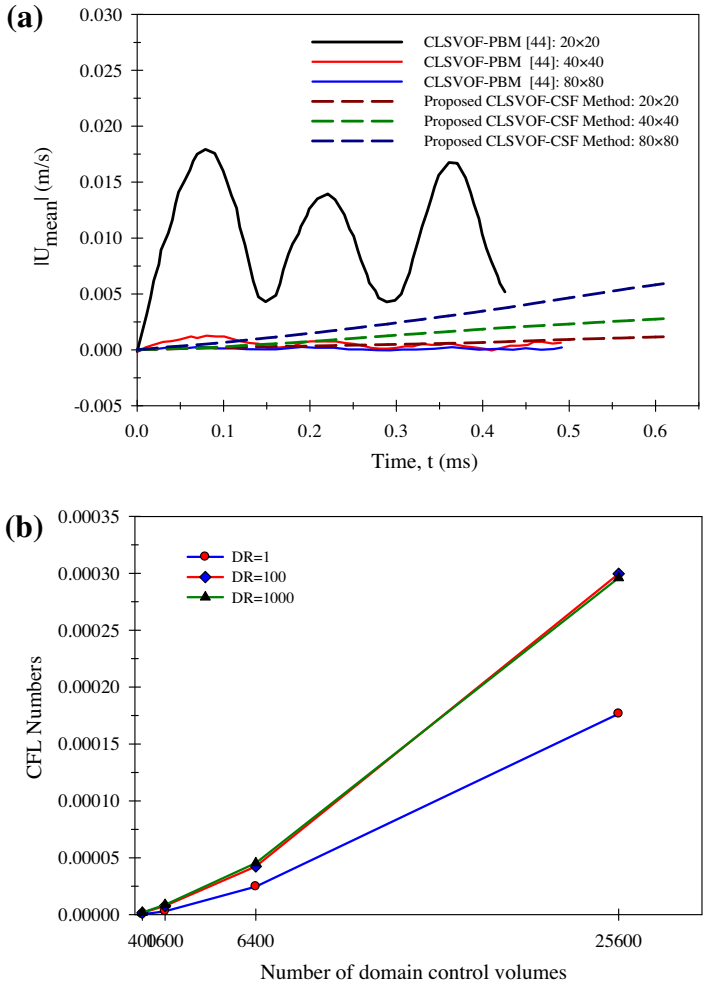

Fig. 5. Comparative study of grid dependence on the mean velocity field (a) CLSVOF-PBM of Wang and Tong [29] and the proposed CLSVOF-CSF method, (b) effect of grid size on spurious current (in terms of CFL number) for various density ratios.

column (H/b) are plotted with respect to the non-dimensional time, $\tau = t(g/a)^{1/2}$ in Fig. 6(a) and (b), respectively. The numerical results obtained from the present CLSVOF-CSF method were compared with the experimental results of Martin and Moyce [52] and numerical results of Zhao et al. [1], Marchandise and Remacle [53], Sun and Tao [54], Sun et al. [55] and Bu and Zhao [56]. Present results show good agreement with the experimental results of Martin and Moyce [52].

5.2.3. Non-linear growth of larger amplitude of Rayleigh–Taylor instability

In this test case, instability of the interface occurs due to the acceleration of a heavier density fluid over a lighter density fluid under the action of gravity. The densities of heavier and lighter fluids are taken as 1.225 kg/m^3 and 0.1694 kg/m^3 respectively. Both the fluids are assumed to be immiscible. For both fluids, a uniform dynamic viscosity of $\mu = 3.13 \times 10^{-3}$ kg/m s is considered. The surface tension coefficient, σ is taken to be 0.001337 N/m. No-slip boundary condition is imposed at the bottom and top boundaries. The free-slip boundary condition is imposed at the left and right side boundaries. Initial pressure distribution in the domain is computed based on the hydrostatic theory. In this test, a rectangular domain size of 1.0 m $\times$ 4.0 m is considered. Interface position at $t = 0$ is patched at the middle of the vertical domain height of, $h/2 = 2.0$ m. The initial interface position is patched in the domain using the expression as

$$y_{\text{int}} = 0.5h + a\cos(kx) \tag{18}$$

where, a is the amplitude of interface and k is the wave number. In the present study, based on Zuzio and Estivalezes [47], the values of a and k are taken to be 0.05 m and 2π, respectively. Zuzio and Estivalezes [47] considered this problem to evaluate the performance of their coupled Level Set/Ghost Fluid method with adaptive grids for two-phase flows. In the present study, the computational domain is discretized using a non-uniform grid size of 128×512. The transient exponential growth of the interfaces obtained using the proposed CLSVOF-CSF method is compared qualitatively with those of Zuzio and Estivalezes [47] in Fig. 7(a) and (b), respectively. The present results show good agreement with [47]. The present results also match well qualitatively with the numerical results of [1,53,57] who considered the same fluid properties and boundary conditions.

5.2.4. Rising of a circular gas bubble inside a stationary liquid column

This problem was evaluated based on the results presented by Zhao et al. [1]. In this test, a circular bubble of diameter, $d = 0.5$ m is initially placed at $(0.5L, 0.25H)$ in a rectangular domain size $L \times H$ of $2d \times 3.4d$ m^2. In this study, the density ratio (DR) of 100 is taken. Initially, zero velocity field and the hydrostatic pressure distribution are specified in the domain. The initial position of the

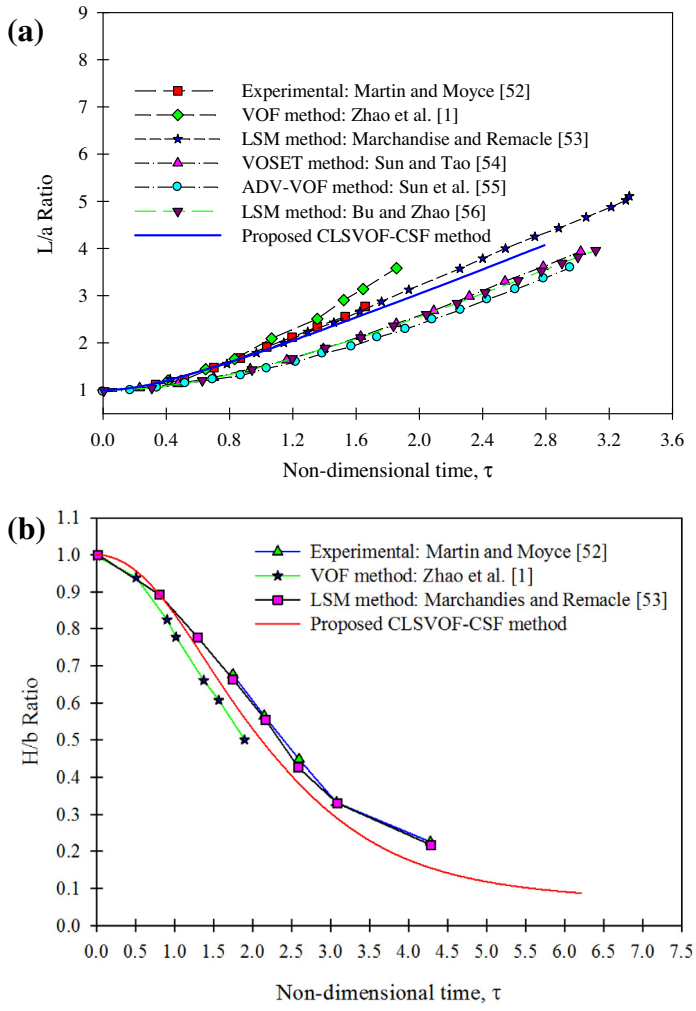

Fig. 6. Comparison of numerical and experimental results of the dam break problem (a) non-dimensional positions of the moving water wave front along the bottom wall (L/a) vs non-dimensional time and (b) non-dimensional vertical column height (H/b) at the left side wall vs non-dimensional time.

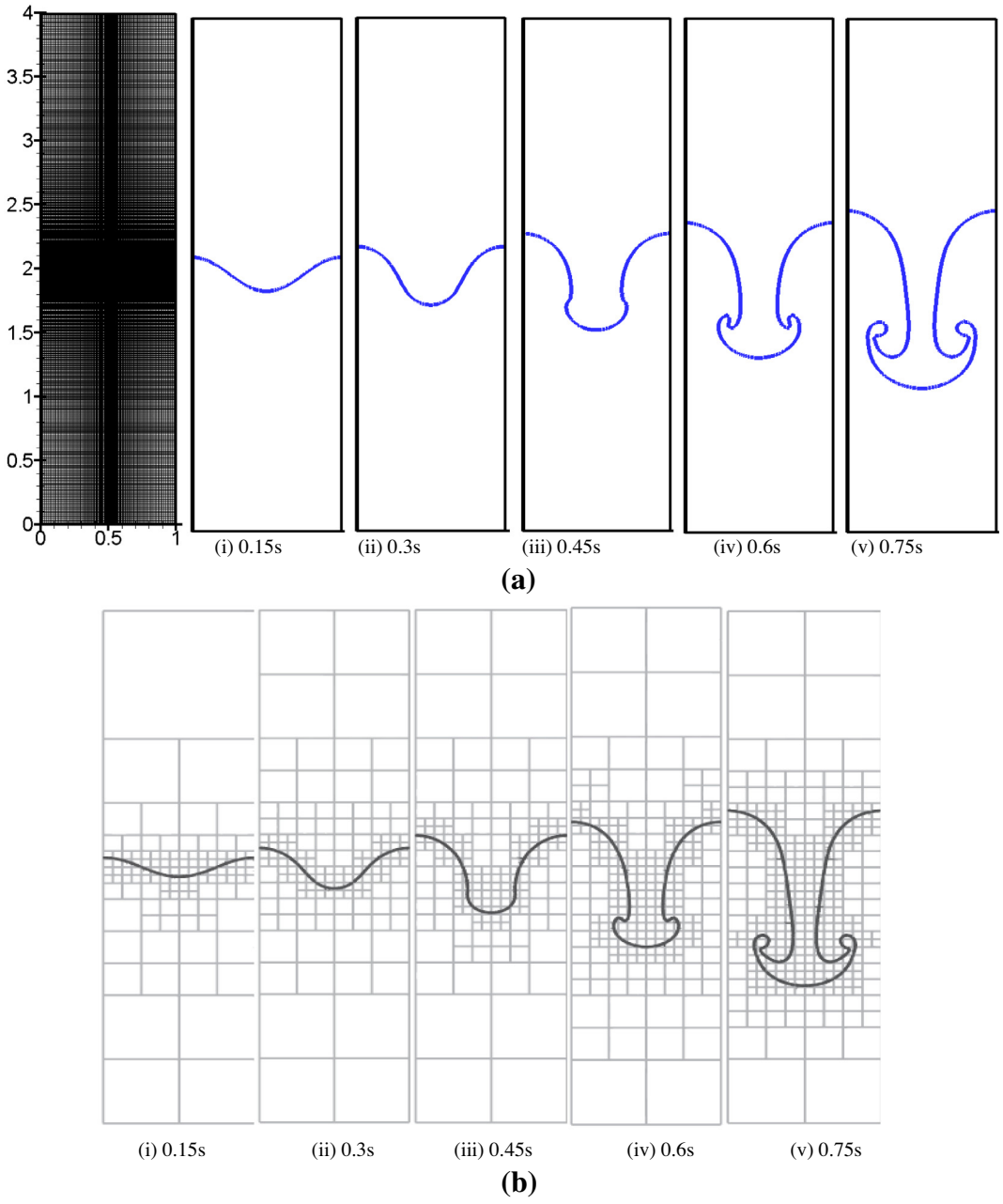

Fig. 7. Comparison of the interface evolution in the Rayleigh–Taylor instability, (a) proposed CLSVOF-CSF method with and (b) Zuzio and Estivalezes [47].

circular bubble in the computational domain and the boundary conditions used to simulate this problem are shown in Fig. 8(a). The domain is discretized using a grid size of 128×218. The non-dimensional time is computed as, $NDT = t\sqrt{\frac{g}{2r}}$, where r is the bubble radius. At DR = 100, the bottom surface of the gas bubble accelerates more quickly compared the top surface of the bubble and then it begins to form a torus [1]. The transient upward rising gas bubble shapes obtained from the present CLSVOF method shown in Fig. 8(b). In Fig. 8(c), the bubble shapes obtained by Zhao et al. [1] are shown for comparison. The bubble shapes obtained from the present study compares very well with those of Zhao et al. [1].

5.3. Evaluation of boiling flow model

In order to evaluate the interfacial phase change model developed for simulating boiling flows, one dimensional Stefan problem and saturated film boiling over a horizontal surface are considered as the standard test cases. In the case of one dimensional Stefan problem, the results obtained from the present study are compared with the exact solutions. For the validation of the model developed for the saturated film boiling flows, the average Nusselt number values obtained from the present study are compared with the values obtained using the correlations available in the literature. The interface topologies obtained for different wall superheats have also been presented.

5.3.1. One-dimensional Stefan problem

This problem is considered as one of the important test cases for the validation of numerical interfacial mass transfer models developed for investigating two-phase flows with phase change [34,39]. Initially, the incompressible vapour and liquid phases are assumed to be at static (or quiescent) equilibrium. In the present study,

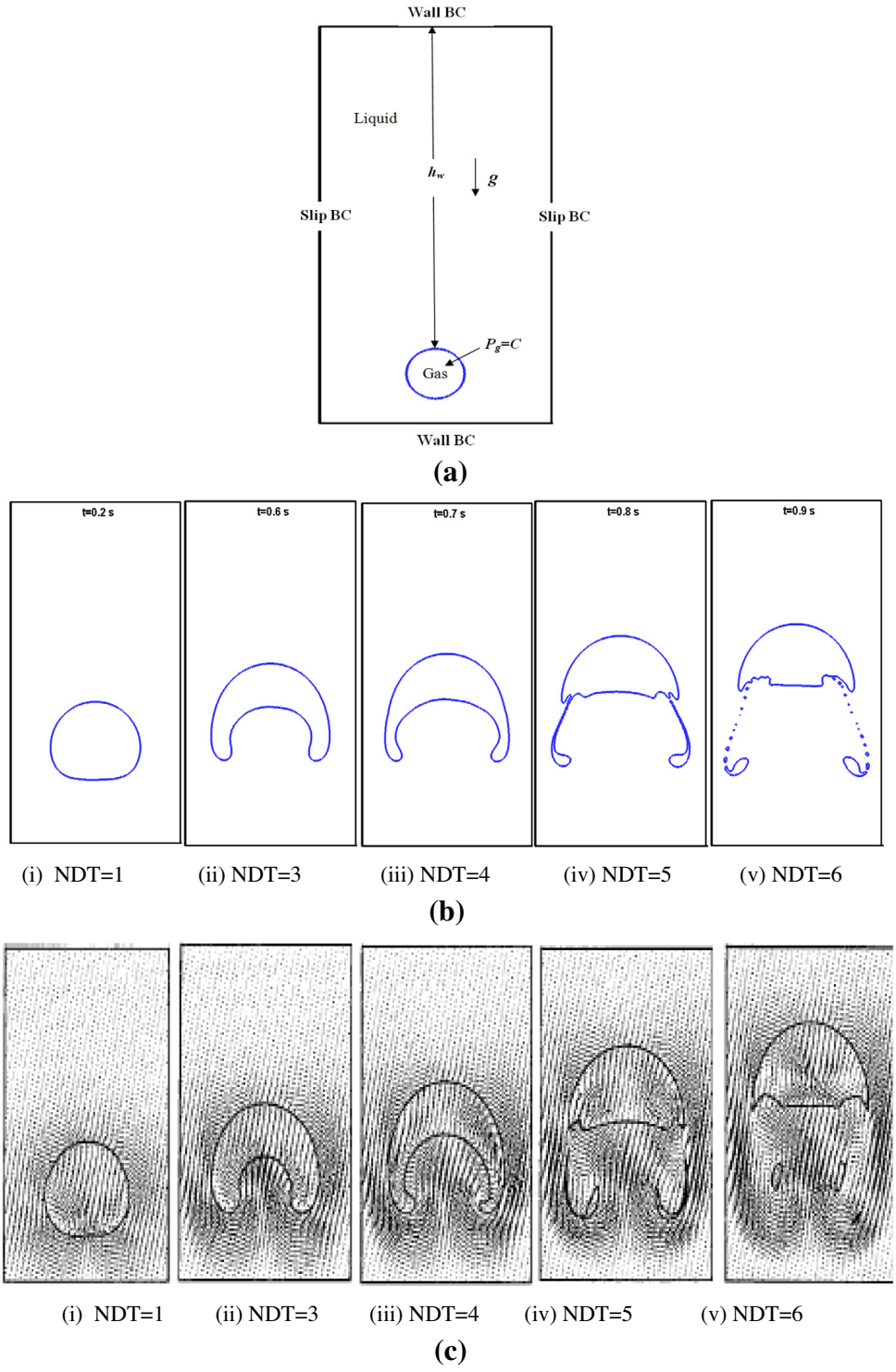

Fig. 8. Rising gas bubble inside a liquid column (a) initial and boundary conditions, (b) interface evolution obtained using the proposed CLSVOF-CSF method and (c) interface evolution of Zhao et al. [1].

uni-directional evaporation of saturated liquid into a superheated vapour is considered to evaluate the phase change model. Fig. 9(a) shows the initial conditions of 1-D Stefan problem. In this study, the wall is maintained at a constant temperature and is higher than the saturation temperature of the fluid. Initially, at time $t = 0$, a thin layer of superheated vapour phase is initialized close to the superheated plane wall. The vapour region is considered as motionless and only conduction is taking place in this region. Continuous conduction heat transfer occurs between the superheated wall and the adjacent quiescent vapour phase. Due to this, a thermal boundary layer develops in the vapour region which drives heat and mass transfer normal to the liquid–vapour interface. Hence, the transient thickness of the superheated vapour layer, $\delta(t)$ increases continuously. The interface moves away from the heated surface due to additional generation of vapour across the interface. The one-dimensional transient heat conduction

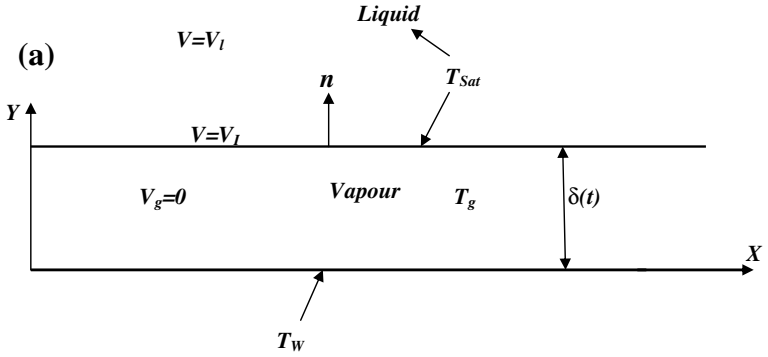

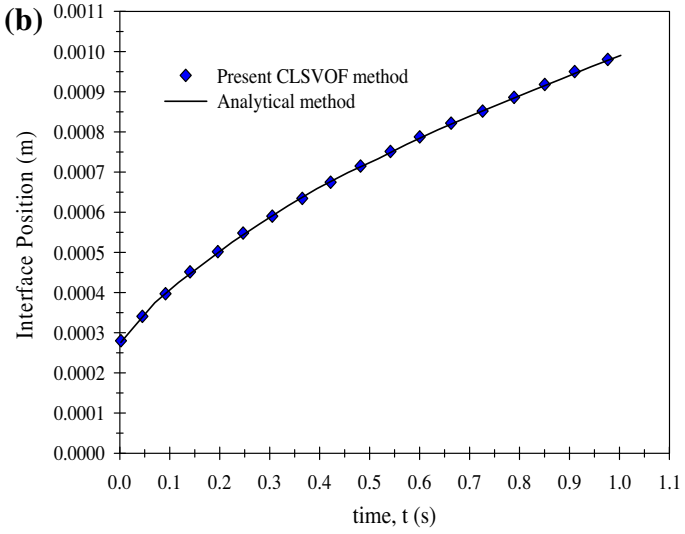

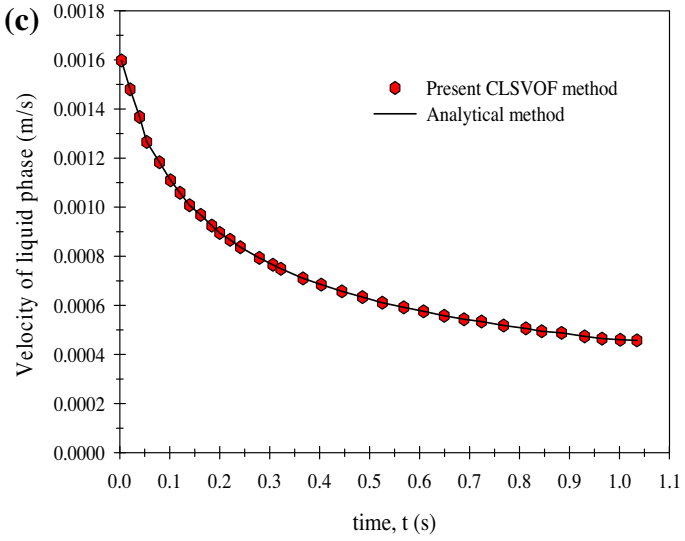

Fig. 9. One-dimensional Stefan problem (a) computational domain, initial and boundary conditions, (b) interface location vs time and (c) the liquid velocity vs time.

equation for the vapour phase in the region of $0 \leqslant y \leqslant \delta(t)$ can be written as

$$\frac{\partial T}{\partial t} = \frac{k_g}{\rho_g Cp_g}\frac{\partial^2 T}{\partial y^2} \tag{19}$$

In the present study, constant wall temperature, T_W is considered at $y = 0$. In the region $y \geqslant \delta(t)$, the liquid phase is considered to be at saturation temperature, T_{Sat}. At the liquid–vapour interface, $y = \delta(t)$, the energy jump conditions is

$$\rho_g \frac{\partial \delta(t)}{\partial t} h_{lg} = -k_g \frac{\partial T}{\partial y}\Big|_{y=\delta(t)} \tag{20}$$

The interfacial velocity field, V_I can be written as

$$V_I = \frac{\partial \delta(t)}{\partial t} = \frac{-k_g \frac{\partial T}{\partial y}\Big|_{y=\delta(t)}}{\rho_g h_{lg}} \tag{21}$$

The normal velocity of the liquid, V_{liq} can be written as

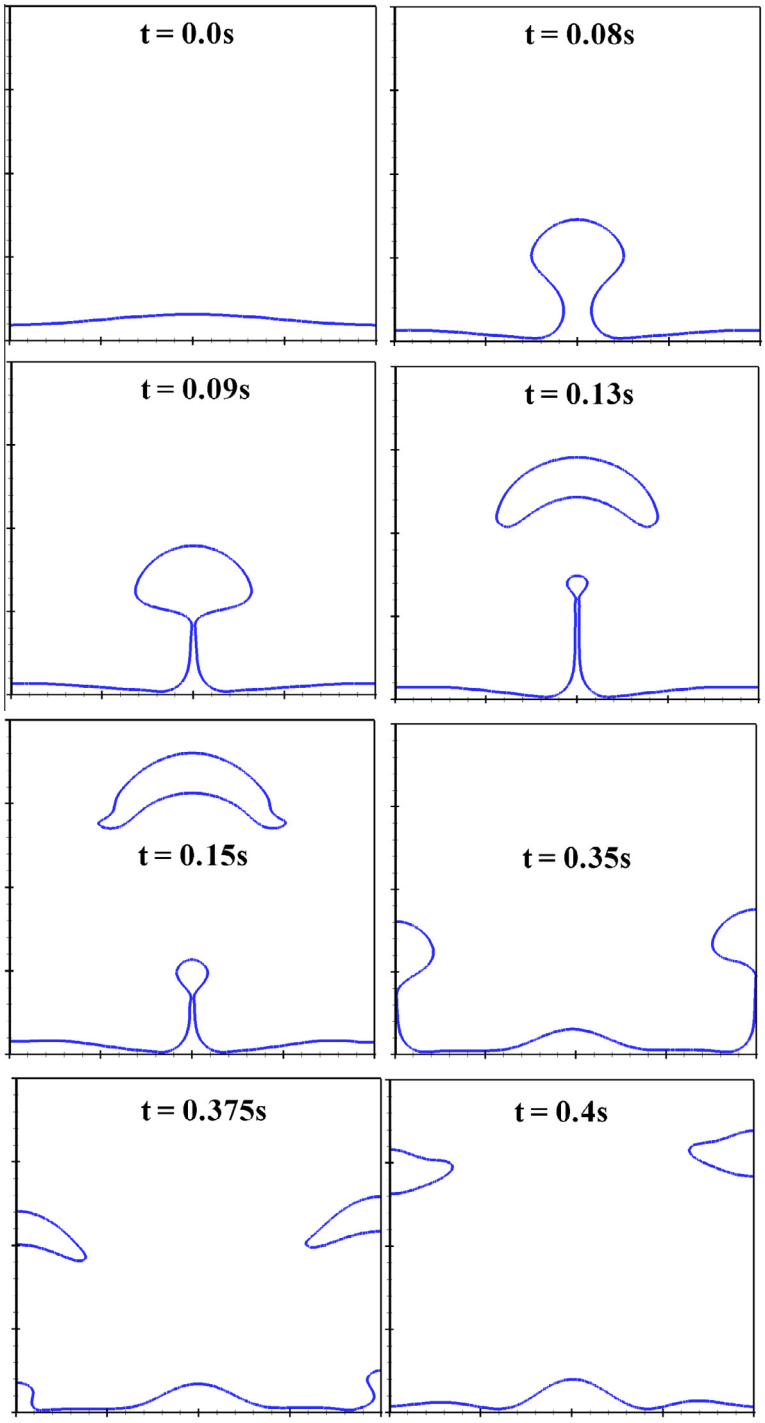

Fig. 10. Periodic bubble release cycle – interface morphology for the near critical water with the wall superheat $\Delta T = 5$ K.

$$V_{liq} = \frac{\partial \delta(t)}{\partial t}\left(1 - \frac{\rho_g}{\rho_l}\right) = V_l\left(1 - \frac{\rho_g}{\rho_l}\right) \tag{22}$$

In the present numerical study, a wall superheat of 25 K is considered. Constant thermophysical properties corresponding to saturated water and its vapour at 1 atm are considered. The thermophysical properties used in the present study are the same that of Welch and Wilson [34]. Even though this problem is one-dimensional, in order to validate the present 2-D phase change model, a two-dimensional domain size of 0.01 m × 0.125 m is considered. In this study, the computational domain is discretized into 4 × 50 cells. Within the superheated vapour region, a linear temperature profile is initialized at time $t = 0$. The time step, Δt used in this test problem is 10^{-5} s. The numerical results obtained from the present CLSVOF method compared with the exact solutions. The transient variation of interface position and the liquid velocity obtained from both numerical study and exact solutions are shown in Fig. 9(b) and (c), respectively. The present numerical results compare very well with the exact solutions.

5.3.2. Saturated film boiling flows over a horizontal flat surface

To evaluate the phase change model developed for the boiling flows, two-dimensional saturated film boiling over a horizontal

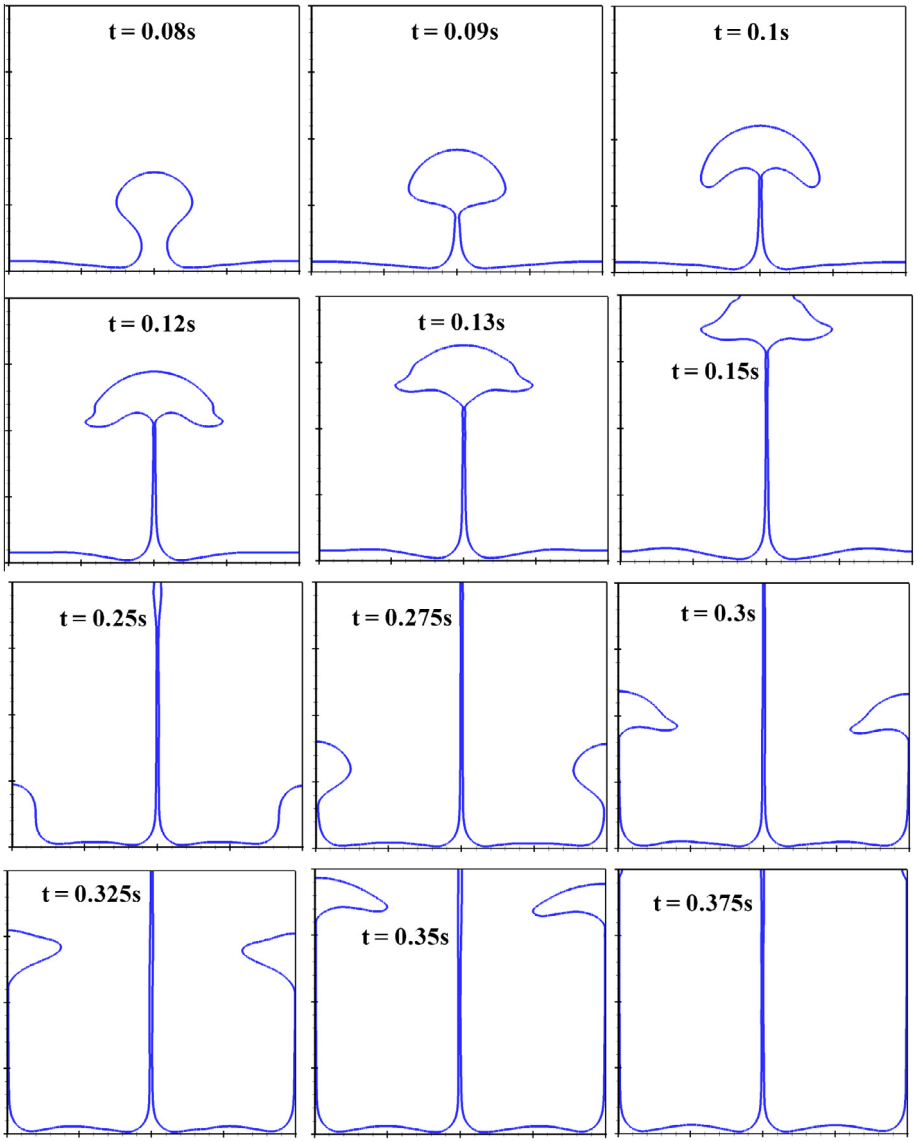

Fig. 11. The formation of a column of vapour jet in the periodic bubble release cycle at the wall superheat $\Delta T = 10$ K.

plane surface is considered as the second test case. This problem was considered as a test case by [23,31–40] to validate the phase change models of boiling flows. In the present study, boiling of water at near critical condition of $T_{Sat} = 646.15$ K and $P_{Sat} = 21.9$ MPa is considered. The thermophysical properties are assumed to be constant as considered by [23,34,40]. In the present study, numerical simulations were carried out for the wall superheats, $\Delta T_{Sup} = 5$ K, 10 K, 15 K and 20 K. Initial characteristic scale parameters used for simulating film boiling flow problems are computed in terms of the thermophysical properties of fluids [23,33,34,36]. The characteristic capillary length (λ), time (t_o) and velocity (u_o) scales are computed as follows:

$$\lambda = \sqrt{\frac{\sigma}{g(\rho_l - \rho_g)}}; \quad t_o = \sqrt{\frac{\lambda}{g}} \quad \text{and} \quad u_o = \frac{\lambda}{t_o} = \sqrt{\lambda g} \tag{23}$$

For two-dimensional film boiling flow problems, the most dangerous Taylor hydrodynamic instability wavelength, λ_d is given as

$$\lambda_d = 2\pi\sqrt{\frac{3\sigma}{g(\rho_l - \rho_g)}} \tag{24}$$

In the present study on saturated film boiling flow, a square computational domain size of $\lambda_d \times \lambda_d$ has been selected. In this problem, initially a thin layer of the superheated vapour film of thickness, $\delta(x)$ is marked underneath a layer of saturated liquid. The initial thin vapour film [23] of thickness, $\delta(x)$ is given as

$$\delta(x) = \frac{\lambda_d}{64}\left(4 + \cos\left(\frac{2\pi x}{\lambda_d}\right)\right) \tag{25}$$

The initial vapour film thickness, $\delta(x)$ is maximum at $x = 0$ (at node) and is minimum at $x = \pm\lambda_d/2$ (at anti-nodes). A thin vapour film completely blankets a superheated horizontal wall from the saturated liquid phase. In this study, a nonuniform grid has been used. Small control volumes are used near the heated wall to capture the temperature gradient more accurately. As alternate bubble formation and departure are expected to occur at node and anti-nodes, smaller cells are used at the middle (node) and left and right sides (anti-nodes) of the square domain. Initially, a linear temperature variation is considered inside the superheated vapour phase. Both the liquid and liquid–vapour interface are assumed to be at a saturation temperature.

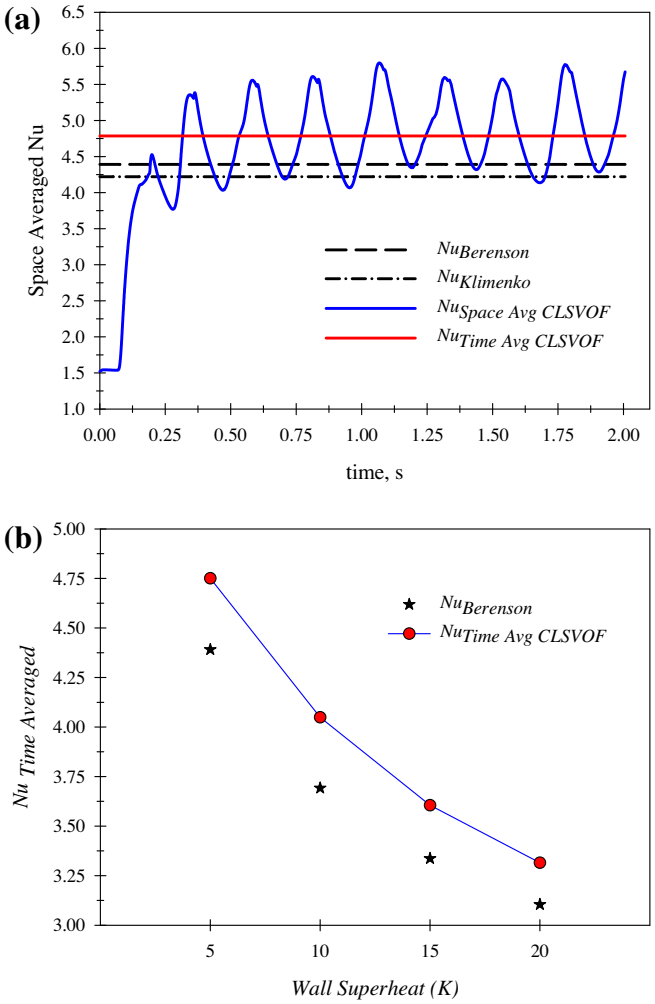

Fig. 12. Comparison of present numerical results with the values of the experimental correlations of Berenson [58] and Klimenko [59] (a) variation of space averaged Nusselt number with time $\Delta T = 5$ K and (b) variation of time averaged Nusselt number with four different wall superheats.

The boundary conditions [23,34,36] used to simulate this boiling flow problem are as follows: No-slip wall with constant temperature is considered at the bottom boundary (at $y = 0$). This boundary condition is specified at the wall as, $u = v = 0$, $T(x, 0) = T_w$; where $T_w = T_{Sat} + \Delta T_{Sup}$. Symmetric boundary condition is imposed at the left and right side of the computational domain. At the top boundary (at $y = H$), outflow conditions is imposed.

The local Nusselt number over the horizontal flat surface, W at $y = 0$ is calculated as,

$$Nu_{\lambda_d} = \frac{\lambda}{(T_W - T_{Sat})}\frac{\partial T}{\partial y}\bigg|_W \tag{26}$$

The space averaged Nusselt number over the horizontal flat heated surface, W at $y = 0$ can be calculated as

$$\overline{Nu}_L = \frac{1}{L}\int_0^L \frac{\lambda}{(T_W - T_{Sat})}\frac{\partial T}{\partial y}\bigg|_W dx \tag{27}$$

The time averaged Nusselt number over the horizontal flat surface can be written as

$$\overline{Nu}_T = \frac{1}{T}\int_0^T \overline{Nu}_L dT \tag{28}$$

A grid independent study was carried out using the nonuniform grid sizes of 100^2, 200^2, 300^2 and 400^2 with a constant wall superheat of 10K and the CFL number, $C = 0.01$. No difference in the interface shape and the space averaged Nusselt number were observed when the grid size is increased from 300^2 to 400^2. Hence, a grid size of 300×300 is selected. The effect of time step, Δt was also investigated with the grid size of 300×300 for the CFL numbers 0.25, 0.1, 0.05 and 0.01 to select a suitable time step. The space averaged Nusselt numbers obtained for these CFL numbers are 1.553, 1.539, 1.537 and 1.535, respectively. The difference in the space averaged Nusselt number is only 0.11% when the CFL number is changed from 0.05 and 0.01. Hence, the CFL number, $C = 0.05$ and a grid size of 300×300 are selected for the numerical investigation of saturated film boiling flow over the flat surface at various wall superheat conditions.

The present numerical model of saturated film boiling flow over a horizontal plane surface was evaluated by comparing the average Nusselt number obtained using the present numerical model with the value obtained from the experimental correlations of Berenson [58] and Klimenko [59]. The space averaged Nusselt number correlation of Berenson [58] is

$$\overline{Nu}_B = 0.425\left(\frac{Gr_g \mathrm{Pr}_g}{Ja}\right)^{\frac{1}{4}} \tag{29}$$

where, non-dimensional parameters, $Gr_g = \left(\frac{g\lambda^3\rho_g(\rho_l-\rho_g)}{\mu_g^2}\right)$; $\mathrm{Pr}_g = \left(\frac{\mu_g Cp_g}{k_g}\right)$ and $Ja = \left(\frac{Cp_g \Delta T_{\mathrm{sup}}}{h_{lg}}\right)$.

Klimenko [59] carried out a generalised analysis of film boiling over the horizontal flat surfaces. The simplified correlation of space averaged Nusselt number given by Klimenko [59] for laminar flow for $Gr_g \leqslant 4.03 \times 10^5$ is

$$\overline{Nu}_K = 0.19(Gr_g \mathrm{Pr}_g)^{\frac{1}{3}} \tag{30}$$

In the present study, the wall superheat of 5 K, 10 K, 15 K and 20 K are considered to analyze the flow and heat transfer characteristics of film boiling over a horizontal flat plate. In saturated film boiling flow a thin layer of vapour film grows into a bubble due to continuous interface mass transfer. Rayleigh–Taylor instability occurs at the interface when the buoyancy driven lighter vapour phase start rising upwards and adjacent heavier liquid phase falls downwards towards the superheated wall. The size of the rising vapour bubble grows further and detached away from the vapour layer. The periodic bubble release cycle of film boiling at the wall superheat of 5 K is shown in Fig. 10. The evaporation of saturated liquid phase normal to the interface generates additional vapour. This continuous vaporisation at the interface prevents direct contact of saturated liquid phase with the superheated wall. At the wall superheat of 10 K, the results show the formation of non-breaking continuous columns of vapour phase at node and anti-nodes (Fig. 11). Similar patterns were also observed at the wall superheat of 17 K by Tomar et al. [23]. At higher wall superheats, after one complete periodic ebullition cycle, the space averaged Nusselt numbers becomes constant due to the formation of stable columns of vapour phase.

The average Nusselt number obtained from the present numerical model and the experimental correlations of Berenson [58] and Klimenko [59] are compared in Fig. 12(a) for the wall superheat of 5 K for a duration of 2.0 s. From these results, it is found that the proposed CLSVOF-CSF method is over predicted by 8.993% and 13.412% with the correlations of Berenson [58] and Klimenko [59], respectively. The previous numerical studies of 2-D film boiling by [23,34,39] have also showed that the space averaged Nusselt number results at 5 K is over predicted as compared to the values obtained using the correlations of Berenson [58] and Klimenko [59]. The time averaged Nusselt numbers obtained from the present CLSVOF-CSF method are compared with the values obtained from the correlation of Berenson [58] in Fig. 12(b) for four wall

superheats considered in the present study. For all the wall superheats, the average Nusselt number obtained from the numerical simulations are higher than the values obtained from the correlation of Berenson [58]. Increase in the wall superheats decreases the space and time averaged Nusselt number. The maximum difference between the present numerical results and the Berenson's correlation [58] is around 10%. Similar trend of numerical study is also found in [23,36,40].

6. Conclusions

In this paper, a new CLSVOF method with multi-directional advection algorithms has been proposed for the phase change problems. The proposed method supports computational domain discretization with non-uniform collocated grids. The SIMPLE algorithm is used for pressure and velocity coupling. The present multi-directional advection method, the geometrical based VOF interface reconstruction and re-initialization of level set function are carried out only once at each time step. This method requires less computational time compared to the operator-splitting algorithm which requires interface reconstruction and re-initialization of level set function twice and thrice for two-dimensional and three-dimensional problems, respectively.

Various test cases were considered to evaluate the performance of the present advection algorithm, surface tension and phase change models. The advection algorithm was evaluated both qualitatively and quantitatively by comparing the available results of slotted disk rotation, shear flow and deformation test cases. In the proposed CLSVOF method, the continuum surface tension force (CSF) approach is implemented for calculating the interfacial surface tension force. The implementation of current CLSVOF-CSF model was evaluated by using the standard two-phase flow test cases of static bubble, dam break, Rayleigh–Taylor instability and rising gas bubble inside a liquid column. In the case of static bubble test case, the proposed model show good agreement with the CLSVOF method with CSF and the PROST based surface tension models investigated by many researchers. The results obtained using the proposed method for the advection and two-phase flow test cases agree very well with the second order accurate operator-splitting algorithm based CLSVOF method. The performance of present phase change model was evaluated using the one-dimensional Stefan problem and the two-dimensional saturated horizontal film boiling flows. The saturated film boiling flow model developed with the proposed CLSVOF model agree well with the experimental correlations and numerical results.

Conflict of interest

None declared.

Acknowledgements

This research work was carried out under the research Grant, No. SR/S3/MERC-0118/2009 sponsored by the Department of Science and Technology (DST), India.

References

[1] Y. Zhao, H.H. Tan, B. Zhang, A high-resolution characteristics-based implicit dual time-stepping VOF method for free surface flow simulation on unstructured grids, J. Comput. Phys. 183 (2002) 233–273.
[2] S.W.J. Welch, Local simulation of two-phase flows including interface tracking with mass transfer, J. Comput. Phys. 121 (1995) 142–154.
[3] S.O. Unverdi, G. Tryggvason, A front tracking method for viscous, incompressible, multi fluid flows, J. Comput. Phys. 100 (1992) 25–37.
[4] S. Osher, J.A. Sethian, Fronts propagating with curvature-dependent speed: algorithm based on Hamilton–Jacobi formulations, J. Comput. Phys. 79 (1988) 12–49.
[5] M. Sussman, P. Smereka, S. Osher, A level set approach for computing solutions to incompressible two-phase flow, J. Comput. Phys. 114 (1994) 146–159.
[6] W.F. Noh, P.R. Woodward, SLIC (simple line interface method), in: A.I. van der Vooren, P.J. Zandbergen (Eds.), Lecture Notes in Physics, vol. 59, Springer-Verlag, Berlin/New York, 1976, pp. 330–340.
[7] D.L. Youngs, Time-dependent multi-material flow with large fluid distortion, in: W. Morton, M.J. Baines (Eds.), Numerical Methods for Fluid Dynamics, Academic Press, New York, 1982, pp. 273–285.
[8] J.E. Pilliod, An analysis of piecewise linear interface reconstruction algorithms for volume-of-fluid methods, M.S. Thesis, University of California, Davis, September, 1992.
[9] Y. Renardy, M. Renardy, PROST: a parabolic reconstruction of surface tension for the volume-of-fluid method, J. Comput. Phys. 183 (2002) 400–421.
[10] J. Lopez, J. Hernandez, P. Gomez, F. Faura, A volume of fluid method based on multidimensional advection and spline interface reconstruction, J. Comput. Phys. 195 (2004) 718–742.
[11] S.V. Diwakar, S.K. Das, T. Sundararajan, A quadratic spline based interface (QUASI) reconstruction algorithm for accurate tracking of two-phase flows, J. Comput. Phys. 228 (2009) 9107–9130.
[12] M. Meier, Numerical and Experimental Study of Large steam-air bubbles injected in a water pool, Dissertation of Doctor of Technical Sciences, Swiss Federal Institute of Technology Zurich, 1999.
[13] D.B. Kothe, W.J. Rider, S.J. Mosso, J.S. Brock, Volume tracking of interfaces having surface tension in two and three dimensions, in: AIAA paper 96-0859, 34th Aerospace Science Meeting and Exhibit, Reno, NV, January, 1996, pp. 15–18.
[14] W.J. Rider, D.B. Kothe, Reconstructing volume tracking methods, J. Comput. Phys. 141 (1998) 112–152.
[15] J. Hernandez, J. Lopez, P. Gomez, C. Zanzi, F. Faura, A new volume of fluid method in three dimensions. Part I: Multidimensional advection method with face-matched flux polyhedra, Int. J. Numer. Methods Fluids 58 (2008) 897–921.
[16] J. Lopez, C. Zanzi, P. Gomez, F. Faura, J. Hernandez, A new volume of fluid method in three dimensions. Part II: Piecewise-planar interface reconstruction with cubic-Bezier fit, Int. J. Numer. Methods Fluids 58 (2008) 923–944.
[17] Y.Y. Tsui, S.W. Lin, A VOF based conservative interpolation scheme for interface tracking (CISIT) of two-fluid flows, Numer. Heat Transfer, Part B: Fundam. 63 (2013) 263–283.
[18] A. Bourlioux, Coupled level set volume of fluid algorithm for tracking material interfaces, in: Proceedings of the Sixth International Symposium on Computational Fluid Dynamics, Lake Tahoe, 15, 1995.
[19] M. Sussman, E.G. Puckett, A coupled level set and volume of fluid method for computing 3D and axisymmetric incompressible two-phase flows, J. Comput. Phys. 162 (2000) 301–337.
[20] G. Son, N. Hur, A coupled level-set and volume-of-fluid method for the buoyancy-driven motion of fluid particles, Numer. Heat Transfer, Part B: Fundam. 42 (2002) 523–542.
[21] M. Sussman, A second order coupled level set and volume-of-fluid method for computing growth and collapse of vapor bubbles, J. Comput. Phys. 187 (2003) 110–136.
[22] G. Son, Efficient implementation of a coupled level-set and volume-of-fluid method for three-dimensional incompressible two-phase flows, Numer. Heat Transfer, Part B: Fundam. 43 (2003) 549–565.
[23] G. Tomar, G. Biswas, A. Sharma, A. Agrawal, Numerical simulation of bubble growth in film boiling using CLSVOF method, Phys. Fluids 17 (112103) (2005) 1–13.
[24] D. Gerlach, G. Tomar, G. Biswas, F. Durst, Comparison of volume-of-fluid methods for computing surface tension-dominant two-phase flows, Int. J. Heat Mass Transfer 49 (2006) 740–754.
[25] M. Sussman, K.M. Smith, M.Y. Hussaini, M. Ohta, R. Zhi-Wei, A sharp interface method for incompressible two-phase flows, J. Comput. Phys. 221 (2007) 469–505.
[26] A.Y. Tong, Z. Wang, A numerical method for capillarity-dominant free surface flows, J. Comput. Phys. 221 (2007) 506–523.
[27] T. Menard, S. Tanguy, A. Berlemont, Coupling level set/VOF/ghost fluid methods: validation and application to 3D simulation of the primary break-up of a liquid jet, Int. J. Multiphase Flow 33 (2007) 510–524.
[28] Z. Wang, J. Yang, B. Koo, F. Stern, A coupled level set and volume-of-fluid method for sharp interface simulation of plunging breaking waves, Int. J. Multiphase Flow 35 (2009) 227–246.
[29] Z. Wang, A.Y. Tong, A sharp surface tension modeling method for two phase incompressible interfacial flows, Int. J. Numer. Methods Fluids 64 (2010) 709–732.
[30] X.F. Yang, A.J. James, J. Lowengrub, X.M. Zheng, V. Cristini, An adaptive coupled level-set/volume-of-fluid interface capturing method for unstructured triangular grids, J. Comput. Phys. 217 (2006) 364–394.
[31] G. Son, V.K. Dhir, Numerical simulation of film boiling near critical pressures with a level set method, ASME J. Heat Transfer 120 (1998) 183–192.
[32] G. Son, V.K. Dhir, Three-dimensional simulation of saturated film boiling on a horizontal cylinder, Int. J. Heat Mass Transfer 51 (2008) 1156–1167.
[33] D. Juric, G. Tryggvason, Computation of boiling flows, Int. J. Multiphase Flow 24 (1998) 387–410.
[34] S.W.J. Welch, J. Wilson, A volume of fluid based method for fluid flows with phase change, J. Comput. Phys. 160 (2000) 662–682.
[35] S.W.J. Welch, T. Rachidi, Numerical computation of film boiling including conjugate heat transfer, Numer. Heat Transfer, Part B: Fundam. 42 (2002) 35–53.

[36] D.K. Agarwal, S.W.J. Welch, G. Biswas, F. Durst, Planar simulation of bubble growth in film boiling in near-critical water using a variant of the VOF method, J. Heat Transfer (ASME) 126 (2004) 329–338.
[37] A. Esmaeeli, G. Tryggvason, Computation of film boiling. Part I: Numerical method, Int. J. Heat Mass Transfer 47 (2004) 5451–5461.
[38] A. Esmaeeli, G. Tryggvason, Computation of film boiling. Part II: Multi-mode film boiling, Int. J. Heat Mass transfer 47 (2004) 5463–5476.
[39] V.H. Gada, A. Sharma, On a novel dual-grid level-set method for two-phase flow simulation, Numer. Heat Transfer, Part B: Fundam. 59 (2011) 26–57.
[40] Y. Tsui, S. Lin, Y. Lai, F. Wu, Phase change calculations for film boiling flows, Int. J. Heat Mass Transfer 70 (2014) 745–757.
[41] J. Lopez, J. Hernandez, Analytical and geometrical tools for 3D volume of fluid methods in general grids, J. Comput. Phys. 227 (2008) 5939–5948.
[42] J.U. Brackbill, D.B. Kothe, C. Zemach, A continuum method for modelling surface tension, J. Comput. Phys. 100 (1992) 335–354.
[43] M.M. Francois, S.J. Cumins, E.D. Dendy, D.B. Kothe, J.M. Sicilian, M.W. Williams, A balance-force algorithm for continuous and sharp interfacial surface tension models within a volume tracking frame work, J. Comput. Phys. 213 (2006) 141–173.
[44] B. Lafaurie, C. Nardone, R. Scardovelli, S. Zaleski, G. Zanetti, Modelling merging and fragmentation in multiphase flows with SURFER, J. Comput. Phys. 113 (1994) 134–147.
[45] B.P. Leonard, A stable and accurate convective modelling procedure based on quadratic upstream interpolation, Comput. Methods Appl. Mech. Eng. 19 (1979) 59–98.
[46] T. Hayase, J.A.C. Humphrey, R. Greif, A consistently formulated QUICK scheme for fast and stable convergence using finite-volume iterative calculation procedures, J. Comput. Phys. 98 (1992) 108–118.
[47] D. Zuzio, J.L. Estivalezes, An efficient block parallel AMR method for two phase interfacial flow simulations, Comput. Fluids 44 (2011) 339–357.
[48] D.J.E. Harvie, D.F. Fletcher, A new volume of fluid advection algorithm: the stream scheme, J. Comput. Phys. 162 (2000) 1–32.
[49] D.J.E. Harvie, D.F. Fletcher, A new volume of fluid advection algorithm: the defined donating region scheme, Int. J. Numer. Methods Fluids 35 (2001) 151–172.
[50] R. Scardovelli, S. Zaleski, Interface reconstruction with least-square fit and split Eulerian–Lagrangian advection, Int. J. Numer. Methods Fluids 41 (2003) 251–274.
[51] S.H. Garrioch, B.R. Baliga, A PLIC volume tracking method for the simulation of two-fluid flows, Int. J. Numer. Methods Fluids 52 (2006) 1093–1134.
[52] J.C. Martin, W.J. Moyce, An experimental study of the collapse of fluid columns on a rigid horizontal plane, Philos. Trans. R. Soc. London, Ser. A 244 (1952) 312–324.
[53] E. Marchandise, J.F. Remacle, A stabilized finite element method using a discontinuous level set approach for solving two phase incompressible flows, J. Comput. Phys. 219 (2006) 780–800.
[54] D.L. Sun, W.Q. Tao, A coupled volume-of-fluid and level set (VOSET) method for computing incompressible two-phase flows, Int. J. Heat Mass Transfer 53 (2010) 645–655.
[55] D.L. Sun, Y.P. Yang, J.L. Xu, W.Q. Tao, An improved volume of fluid method for two-phase flow computations on collocated grid system, J. Heat Transfer 133 (2011) 1–8.
[56] L. Bu, J. Zhao, Numerical simulation of the water bubble rising in a liquid column using the combination of level set and moving mesh methods in the collocated grids, Int. J. Therm. Sci. 59 (2012) 1–8.
[57] J. Lopez, J. Hernandez, P. Gomez, F. Faura, An improved PLIC-VOF method for tracking thin fluid structures in incompressible two-phase flows, J. Comput. Phys. 208 (2005) 51–74.
[58] P.J. Berenson, Film-boiling heat transfer from a horizontal surface, J. Heat Transfer 83 (1961) 351–358.
[59] V.V. Klimenko, Film boiling on a horizontal plate-new correlation, Int. J. Heat Mass Transfer 24 (1981) 69–79.